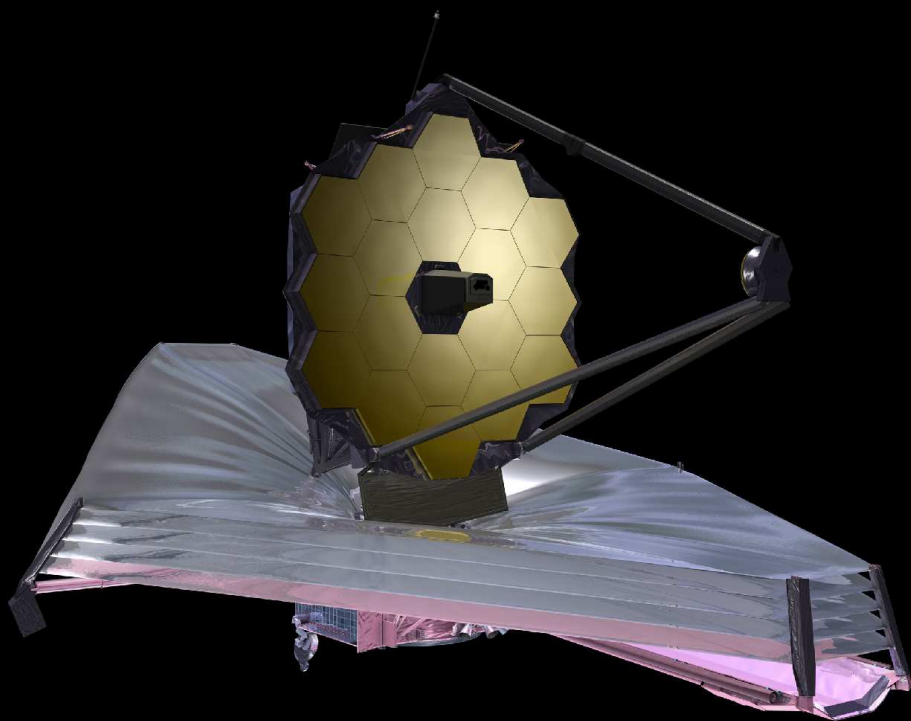


Update of JWST IDS GTO Science Program: Time Domain Science, Cluster Lensing & Caustic Transits

Rogier Windhorst (ASU) — JWST Interdisciplinary Scientist

GTO team: T. Ashcraft, S. Cohen, R. Jansen, V. Jones, B. Joshi, D. Kim, B. Smith, F. Timmes, C. White (ASU), M. Alpaslan (NYU), D. Coe, N. Grogin, N. Hathi, A. Koekemoer, N. Pirzkal, A. Riess, R. Ryan, L. Strolger (STScI), C. Conselice, I. Smail (UK), W. Bricken, J. Condon, W. Cotton, K. Kellermann, R. Perley (NRAO), J. Diego, T. Broadhurst, (Spain), S. Driver, R. Livermore, M. Marshall, A. Robotham, S. Wyithe (OZ), K. Duncan, H. Rottgering (Leiden), S. Finkelstein, R. Larson (UT), G. Fazio, M. Ashby, P. Maksym (CfA), B. Frye, M. Rieke, C. Willmer (UofA), H. Hammel (AURA), G. Hasinger (ESA), A. Kashlinsky, S. Milam, A. Straughn (GSFC), W. Keel (U-AL), P. Kelly (U-MN), P. S. Rodney (U-SC), M. Rutkowski (MNSU), H. Yan (U-MO), A. Zitrin (Israel).



- Today, the JWST science remains as compelling as it was ~ 20 years ago.
- In fact, the JWST science is far more exciting today than we could have imagined or planned for ~ 20 years ago.

Talk at the JWST SWG, STScI, Baltimore; 15 Nov. 2019

(1) Outline & Conclusions

(2) JWST Time-Domain Field in the NEP Continuous Viewing Zone:

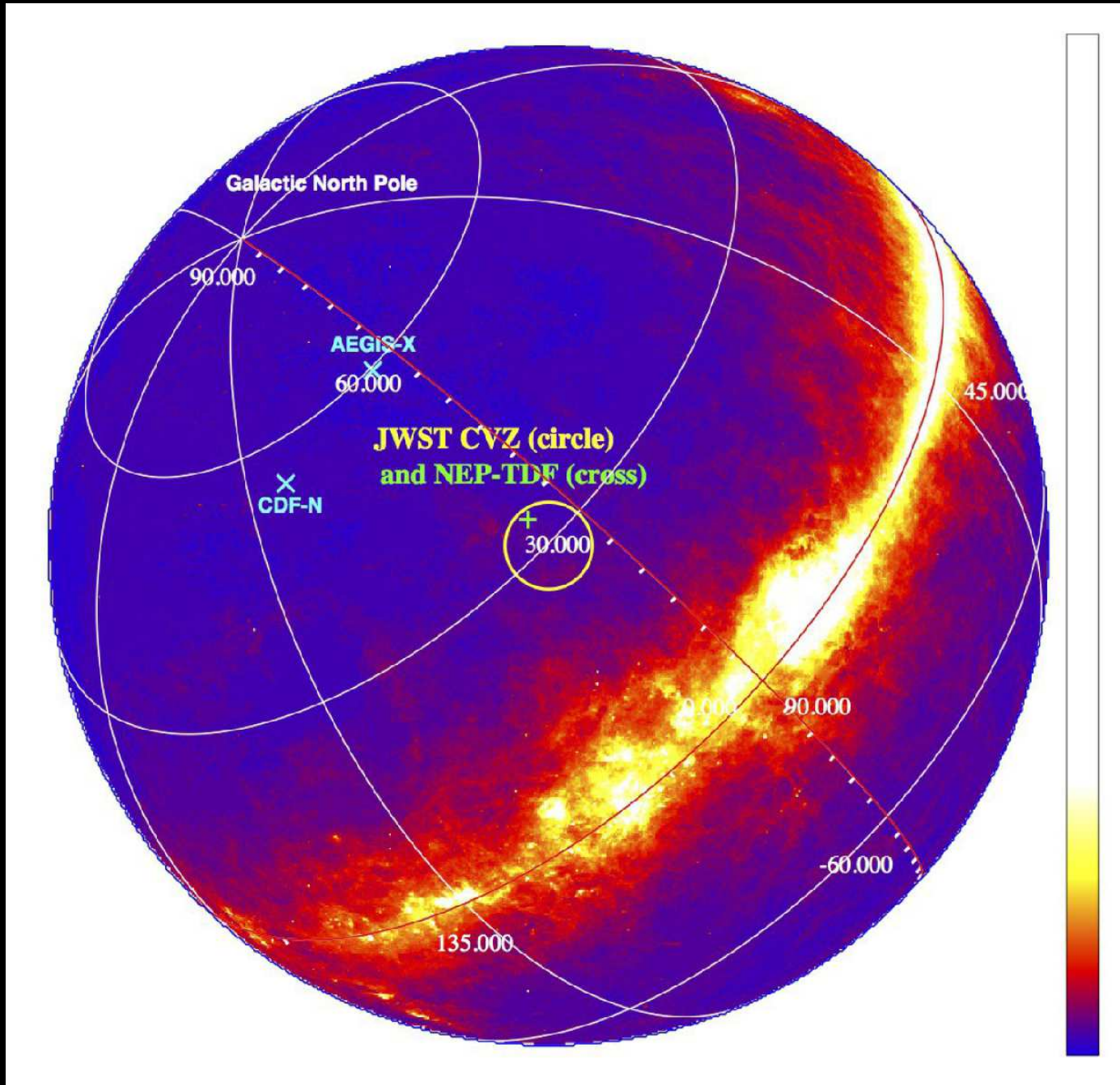
- Weak AGN Variability (*e.g.*, SF–AGN connection; support LyC studies);
- Very high redshift supernovae incl Pair Instability Supernovae (PISN).
- Dark sky in NEP TDF: CIB-fluctuations constrain First Light sources.
- The JWST North Ecliptic Pole CVZ area will be a Community Field for Time Domain science over 5–14 years (max JWST propellant life): first JWST epoch public rightaway + data products ASAP.

(3) We are getting the best possible (ground-based) data before JWST flies on some of the best lensing clusters.

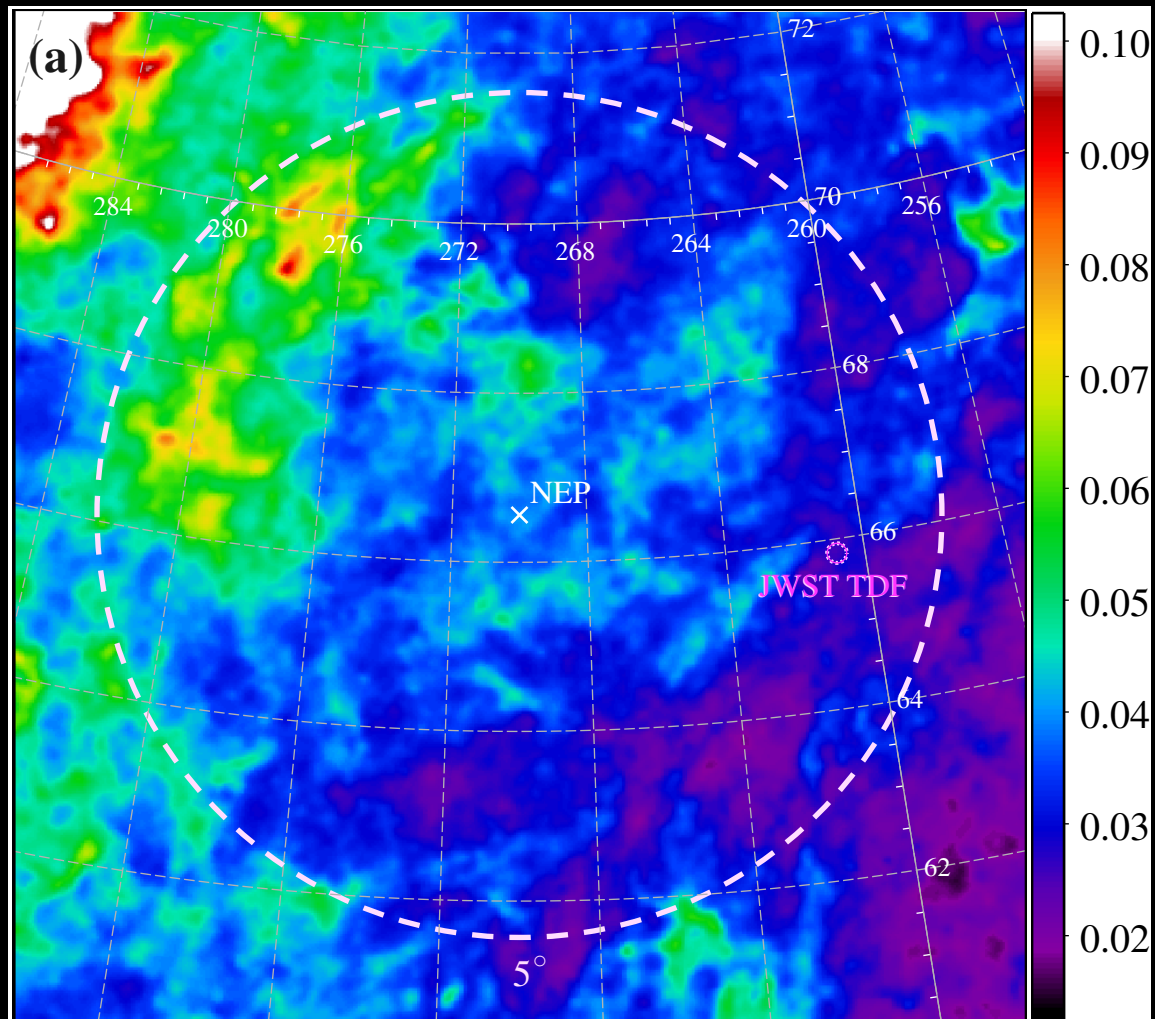
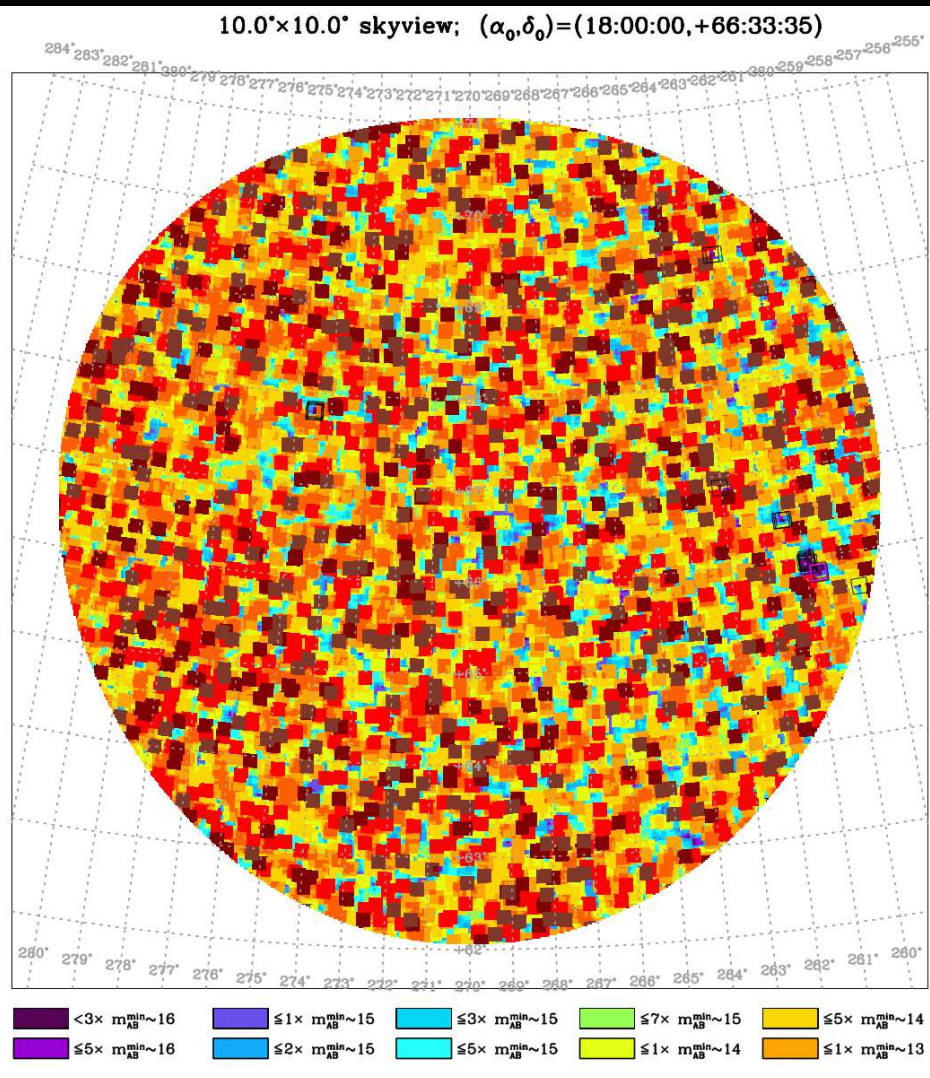
Monitor these clusters for possible JWST caustic transits (of Pop III stars and their stellar-mass black hole accretion disks at $z \gtrsim 7$).

- Limits to the SKY-SB from First Stars & Stellar-Mass Black Holes \implies
- JWST may detect Pop III objects directly monitoring $\gtrsim 3$ lensing clusters.

(2) JWST Continuous Viewing Zones (CVZs): North & South Ecliptic Poles.



Location of the JWST NEP TDF in our Galaxy ($b^{II} \simeq 33^\circ$).

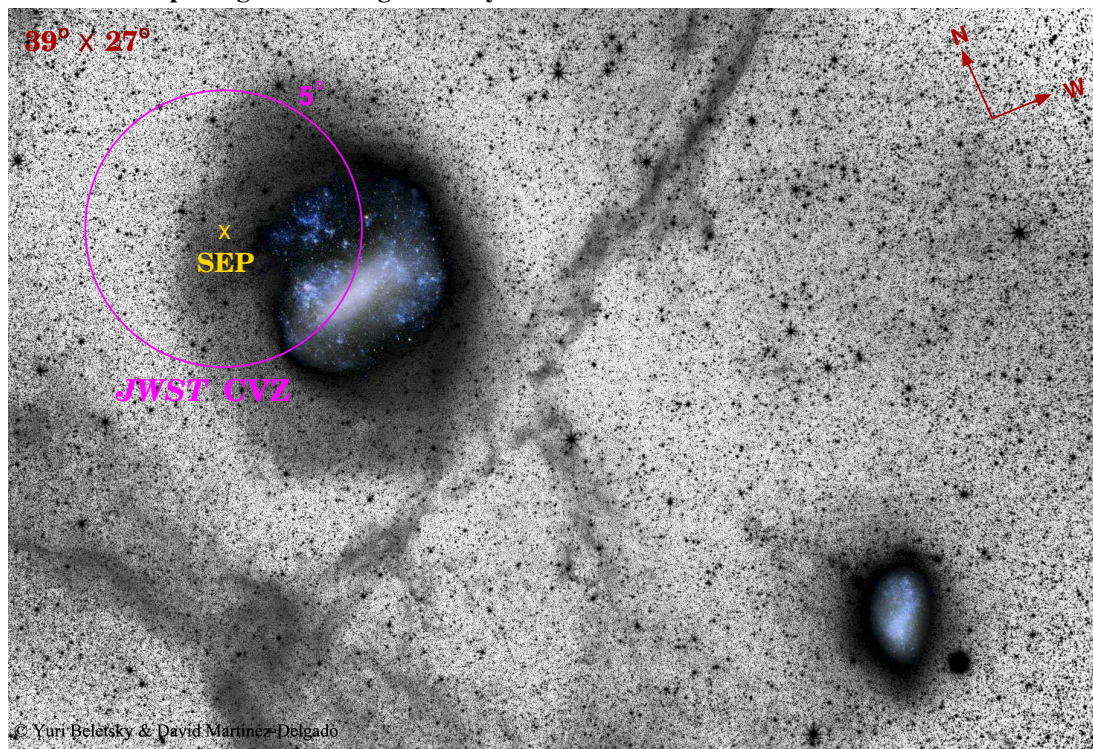


[LEFT]: *WISE* $4\mu\text{m}$ bright star density: Very few regions (purple) without bright stars ($AB \lesssim 16$) to minimize persistence in JWST images

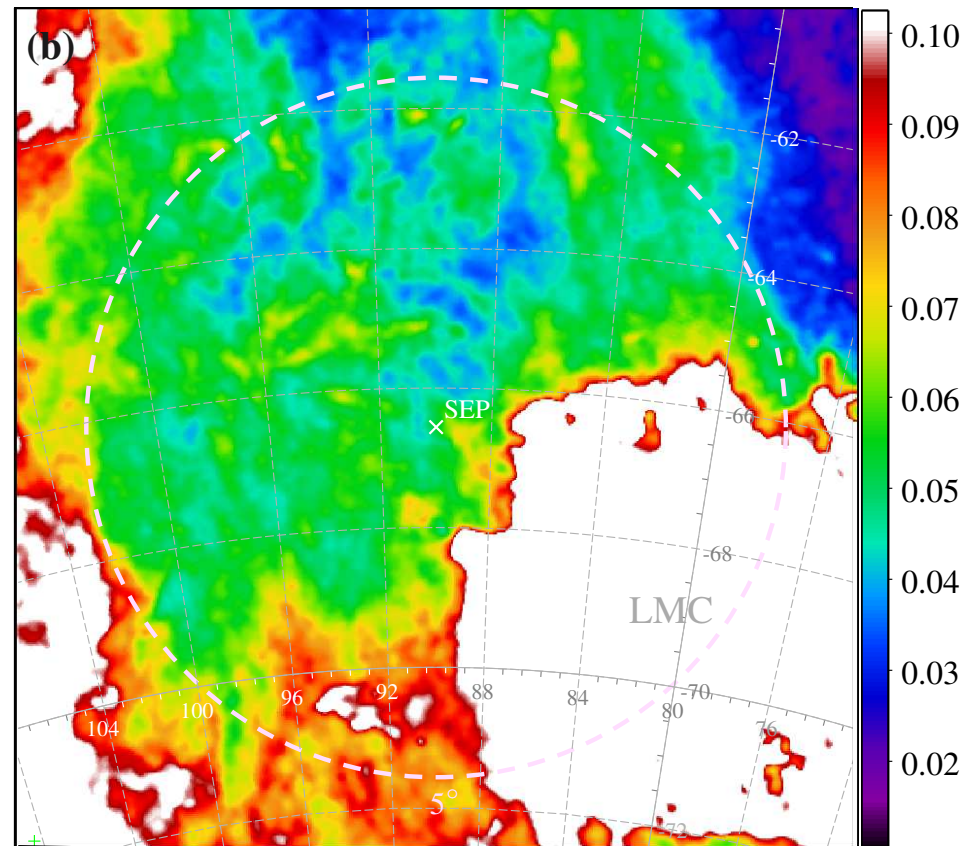
(Jansen & Windhorst, 2018, PASP, 130, 124001).

[RIGHT]: $E(B-V)$ map (Schlegel⁺ 1998) in same NEP-region ($b^{II} \simeq 33^\circ$).
Cleanest $r=7'$ region for JWST has modest extinction: $E(B-V) \lesssim 0.028^m$.

Deep Image of the Magellanic System with southern JWST CVZ indicated.



Besla, G., Martínez-Delgado, D., van der Marel, R., Beletsky, Y., et al. 2016, ApJ 825, 20



[LEFT] Map of LMC+SMC (Besla et al. 2016, ApJ, 825, 20).

[RIGHT]: $E(B-V)$ map (Schlegel et al. 1998) in SEP-region.

- SEP will be good for CVZ studies of LMC and its outskirts.
- SEP/LMC can be a counter-target for NEP surveys: offsets accumulated angular momentum, and so help save JWST propellant/lifetime.
- JWST should observe and monitor bottom of IMF in LMC at SEP.

Table 1: JWST NEP Time-Domain Field multiwavelength community investment

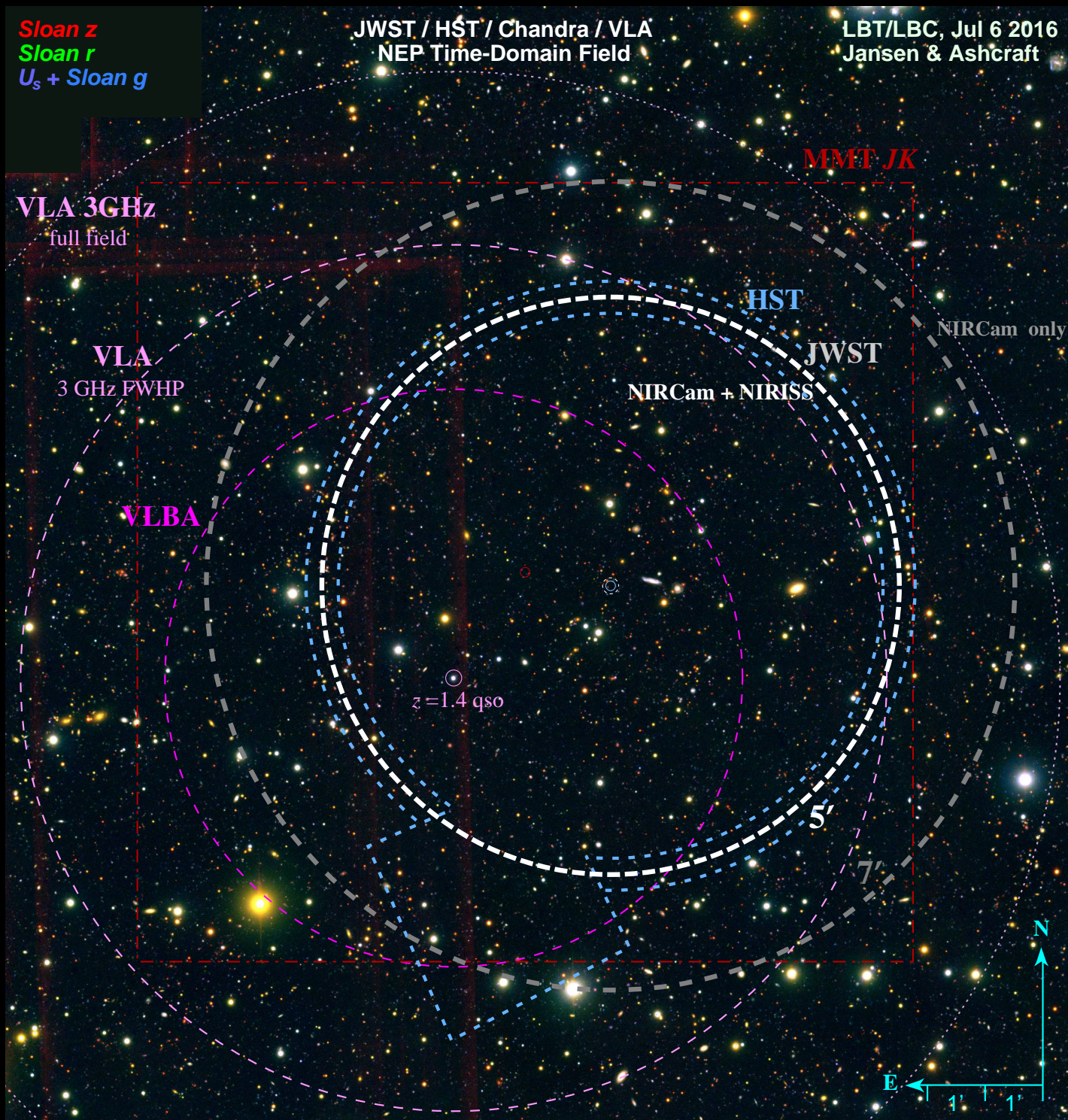
Telescope	PI	Status	Depth
<i>NuSTAR</i> 3–24 keV	F. Civano	approved	585 ks; >50 cts
<i>Chandra</i> /ACIS-I 0.2–10 keV	W.P. Maksym	in hand; 145 sources	300 ks; $\sim 4.1 \times 10^{-16}$ cgs
”	”	in progress / approved	240 ks / 360 ks
<i>XMM-Newton</i> 0.5–2.0 keV	M. Ward / N. Cappelluti	proposed	600 ks; 3×10^{-16} cgs
<i>HST</i> /WFC3+ACS F275W,F435W,F606W	R.A. Jansen	in hand; inner $r < 5'$ only GO 15278	36 CVZ orbits; $m \sim 27.2, 28.2, 29$ mag
”	”	proposed; annulus to $r \sim 14.2'$	52 CVZ orbits
<i>LBT</i> /LBC $U_{sp}grz$	R.A. Jansen	in hand; wide-field	5 hrs; $m \sim 26.5$ –25.5 mag
”	”	in hand; 2nd epoch + i	5 hrs; $m \sim 26.5$ mag
<i>Subaru</i> /HSC $giz, nb816, nb921$	G. Hasinger / E. Hu	in hand; wide-field	5 hrs; $m \sim 25.5$ –25.1 mag
<i>GTC</i> /HiPERCAM $ugriz$	V. Dhillon	proposed; narrow-field	33 hrs; $m \sim 28$ mag
<i>TESS</i> (0.6–1.0 μ m bandpass)	G. Berriman & B. Holwerda	in progress; ultra wide-field	357 days; low-SB (tbd)
<i>MMT</i> /MMIRS (img) $YJHK_s$	C.N.A. Willmer	in hand	60 hrs; $m \sim 23$ –24
<i>JWST</i> /NIRCam+NIRISS 0.8–5 μ m + 1.75–2.23 μ m	R.A. Windhorst / H.B. Hammel	<i>guaranteed time</i> GTO #1176, #1255	~ 49 hrs total; $m < 29$ –28.5 mag
<i>JCMT</i> /SCUBA-2 850 μ m	I. Smail / M. Im	in progress; ≥ 59 sources	31 hrs; rms ~ 1 mJy
<i>SMA</i> 0.87 mm	G. Fazio	approved pilot; lost to protests	37.5 hrs; rms ~ 0.9 mJy
<i>IRAM</i> /Nika2 1.2, 2 mm	S.H. Cohen	in progress	30 hrs; rms ~ 2 mJy
<i>VLA</i> 3(2–4) GHz	R.A. Windhorst / W. Cotton	in hand; ~ 2500 sources	47 hrs; rms ~ 0.9 μ Jy
<i>VLBA</i> 4.7 GHz	W. Brisken	in hand; ~ 200 targets	147 hrs; rms ~ 3 μ Jy
<i>LOFAR</i> 150 MHz	R. van Weeren	approved	75 hrs; rms ~ 25 μ Jy
<i>J-PAS</i> (56 narrow-band spectroh.)	S. Bonoli / R. Dupke	in hand; ultra-wide field	48 hrs; $m \sim 21.5$ –22.5 mag
<i>MMT</i> /Binospec (mos)	C.N.A. Willmer	in hand; 582 spectra/552 redshifts	18 hrs; $m \sim 22.5$ –24 mag
”	”	approved	8 hrs; $m \sim 22.5$ –24 mag
<i>MMT</i> /MMIRS (mos)	C.N.A. Willmer	approved	$m < 22, z > 0.4$

Panchromatic JWST NEP TDF data available or in progress as of Fall 2019.
IDS GTO pgm focus on ground-based data supporting the JWST NEP TDF.

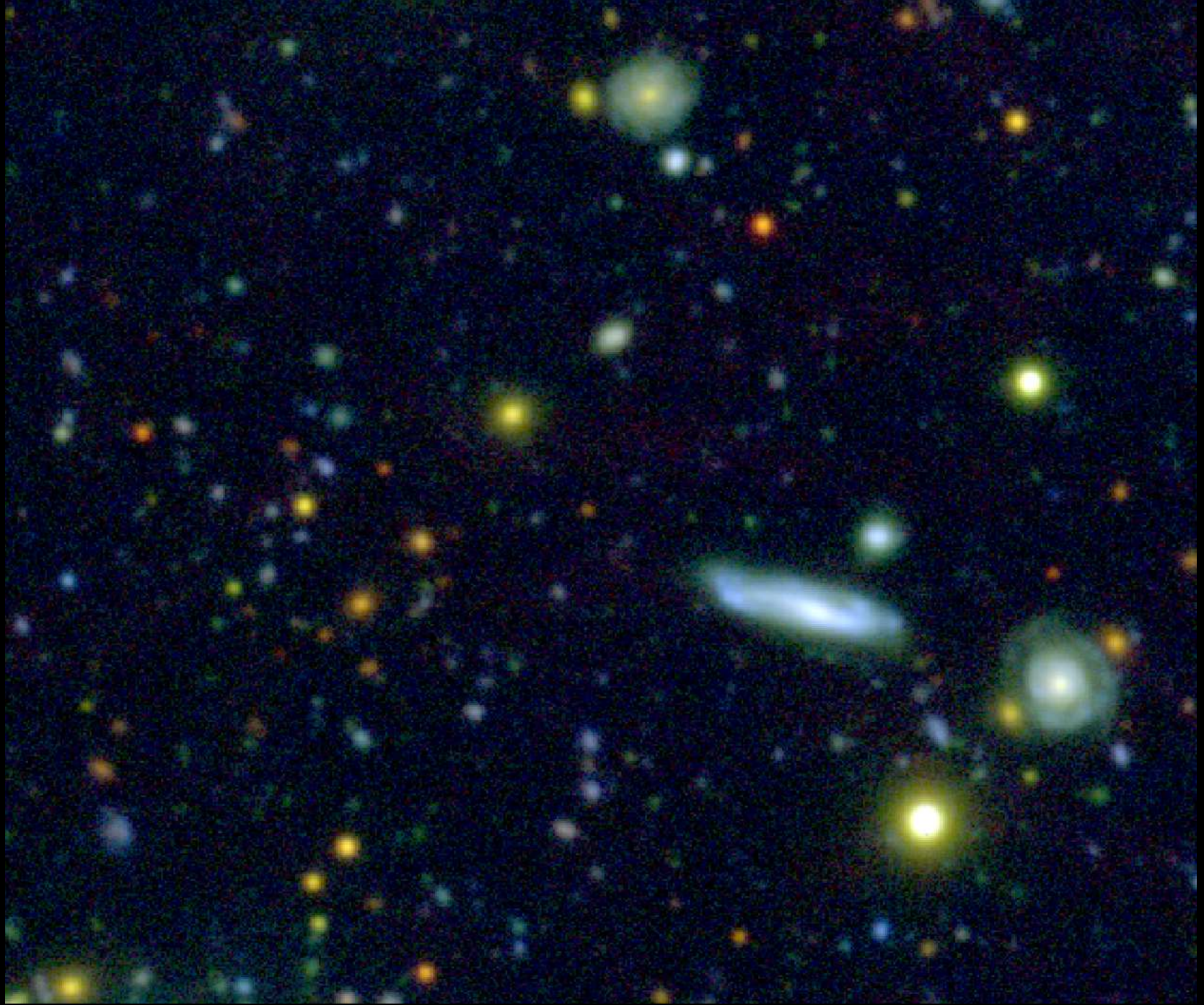
Sloan z
Sloan r
U_s + Sloan g

JWST / HST / Chandra / VLA
NEP Time-Domain Field

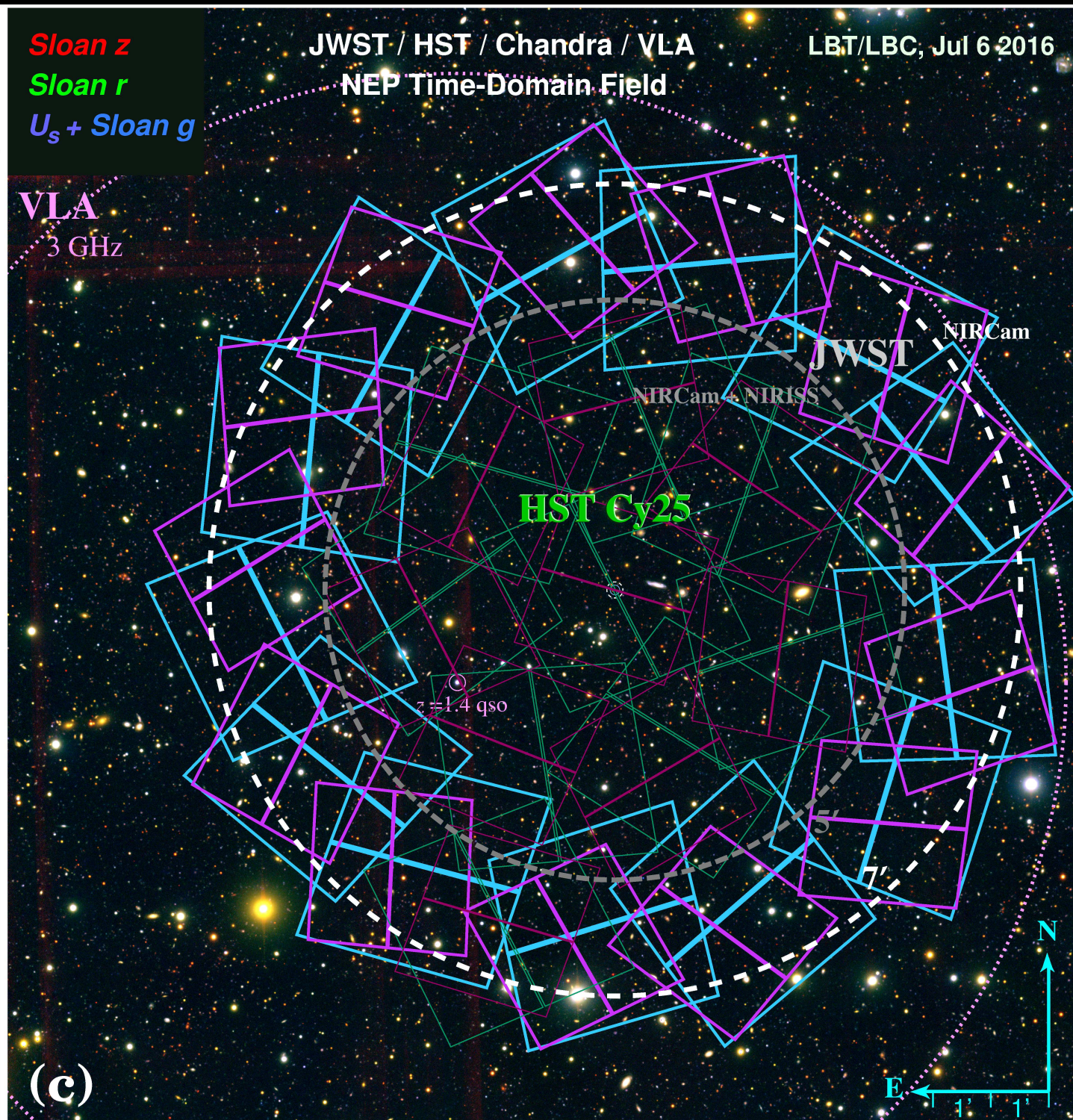
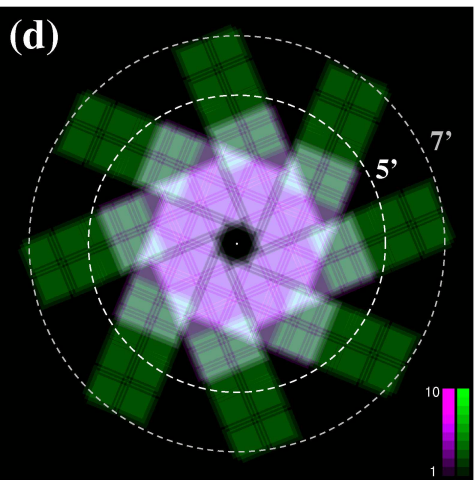
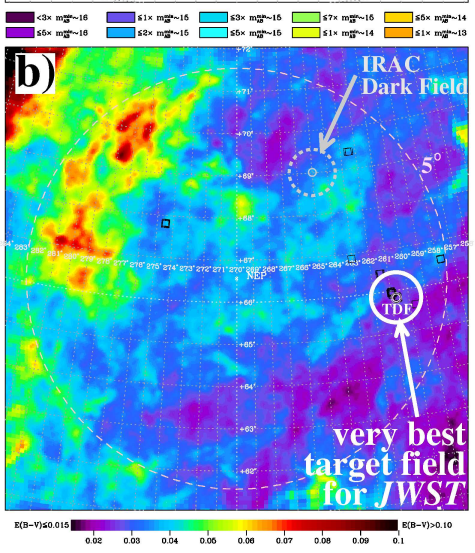
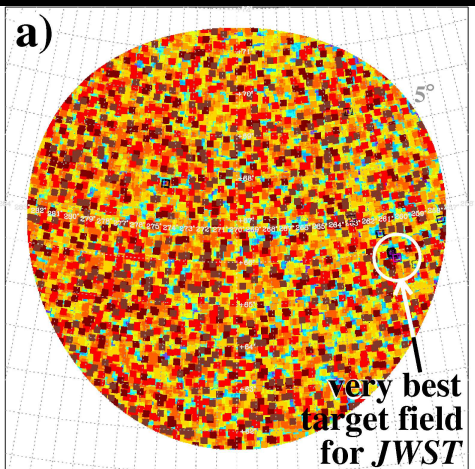
LBT/LBC, Jul 6 2016
Jansen & Ashcraft



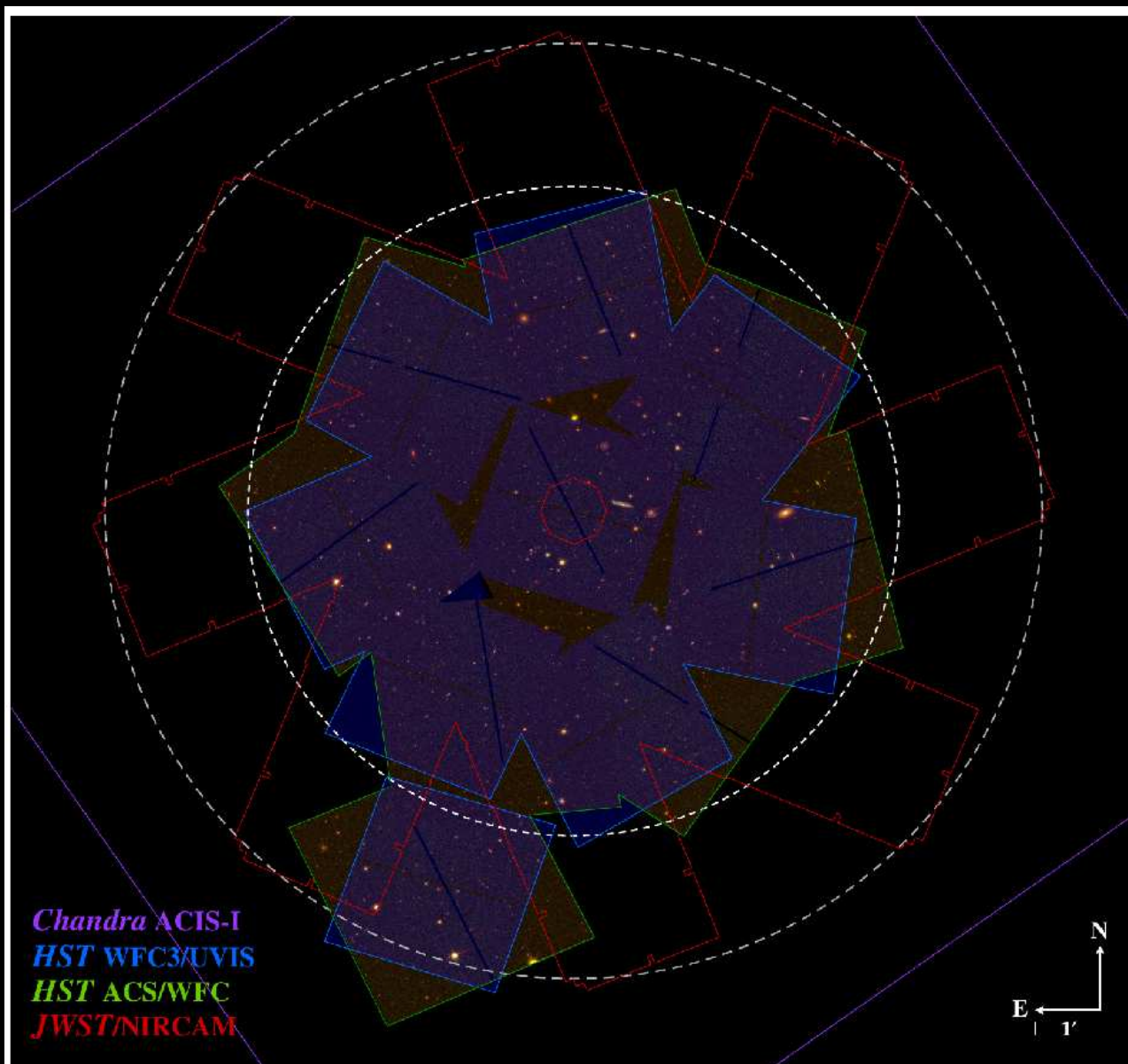
$r=7'$ JWST NEP Time-Domain Field is free of bright ($AB \lesssim 16$) stars.



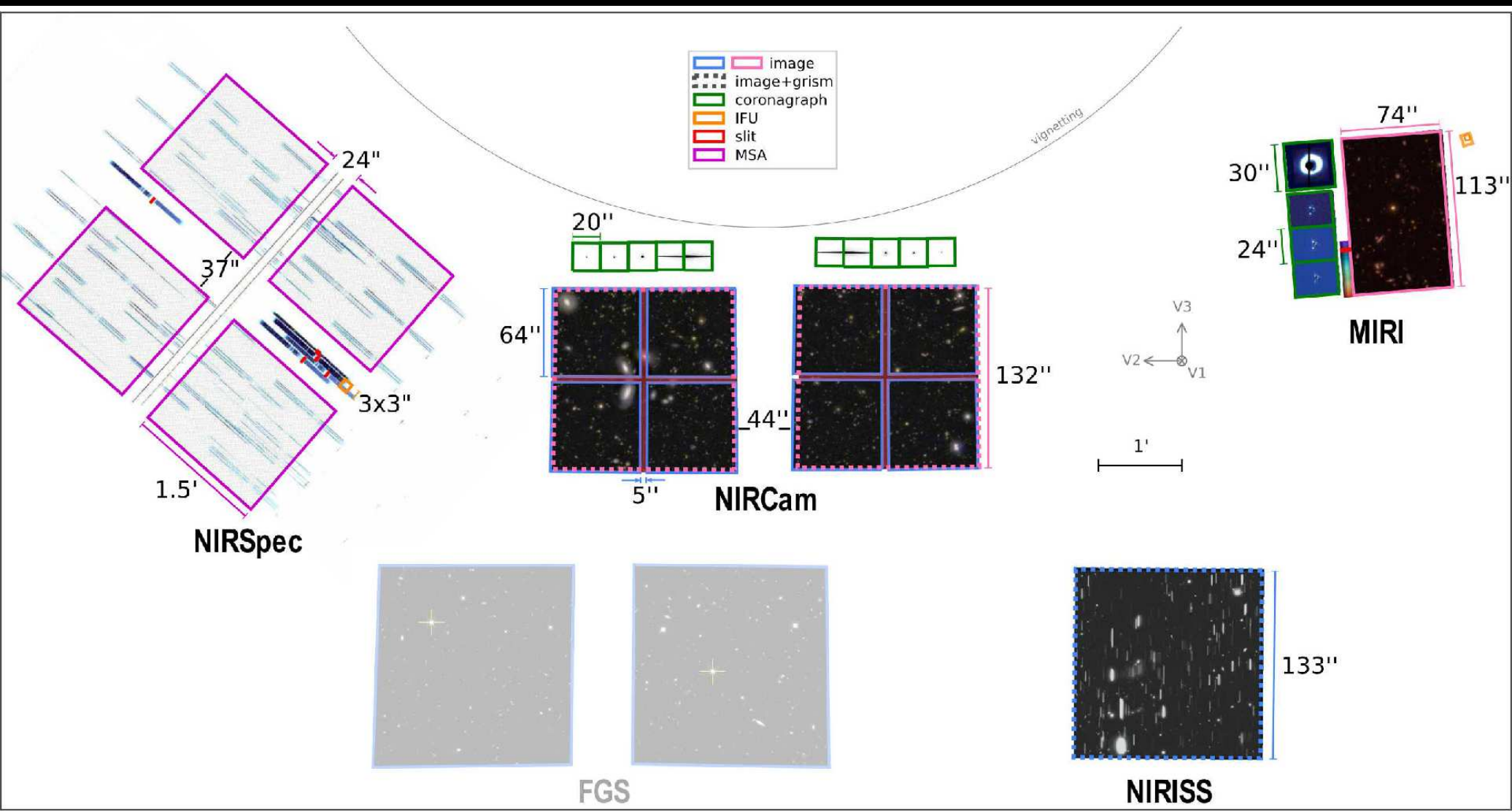
At $r \lesssim 7'$, JWST NEP TDF is a clean extragalactic survey field (LBT).
To $AB \lesssim 26$ mag, get many faint Galactic brown dwarfs and high- z dropouts.



JWST NEP TDF with HST Cy \gtrsim 25 ACS+WFC3 outlay overlaid.

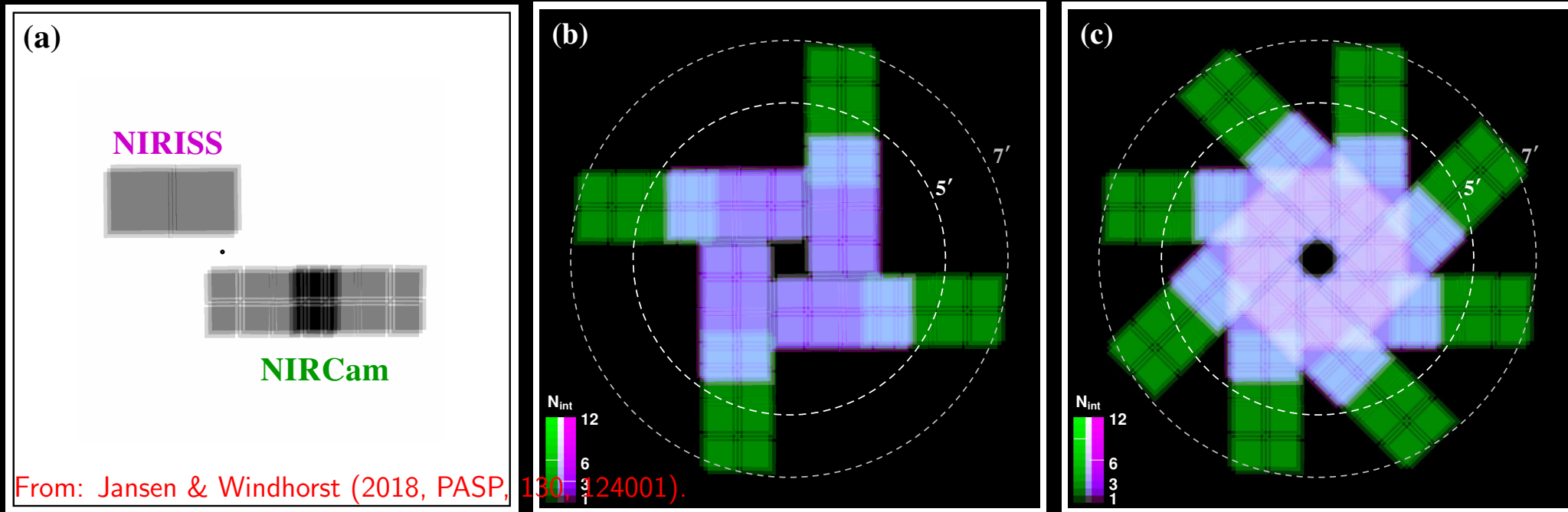


(2) NIRCam + NIRISS-parallels optimally cover the JWST NEP TDF.



- Most-used JWST instrument pairs implemented for science parallels.
- CVZ enables overlapping *dark-sky* NIRCam + NIRISS-parallel mosaics.
- JWST NIRISS grism science (parallel to NIRCam) is essential!

Exposure Maps of NEP JWST-Windmill & GO-Extensions:



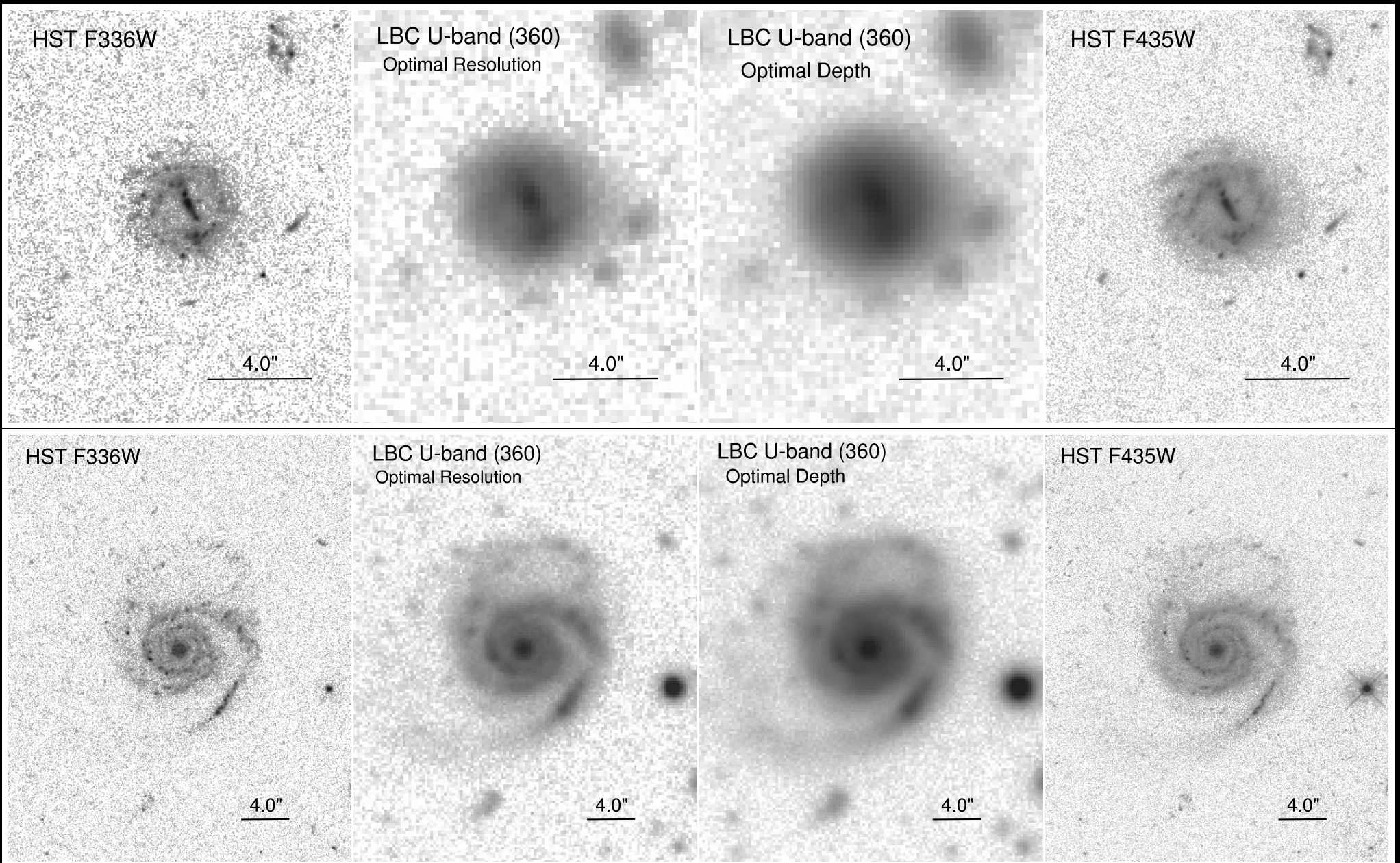
[LEFT]: Exposure map of two contiguous areas: NIRCams primary (green) + NIRISS parallel grism (purple), observable at any PA.

[MIDDLE]: Same with $\Delta PA = 90 + 180 + 270^\circ$ added: our 50-hr GTO plan.

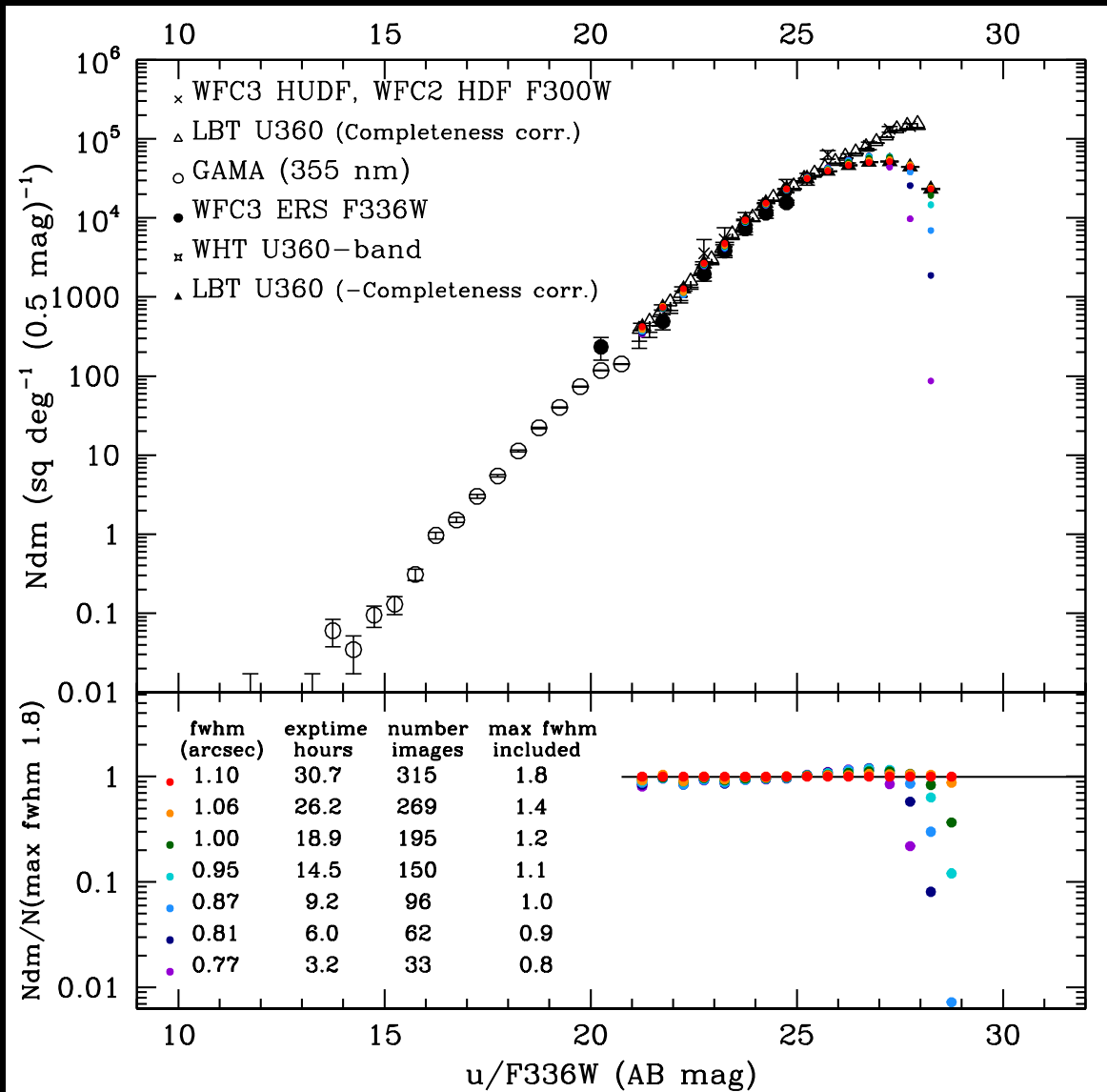
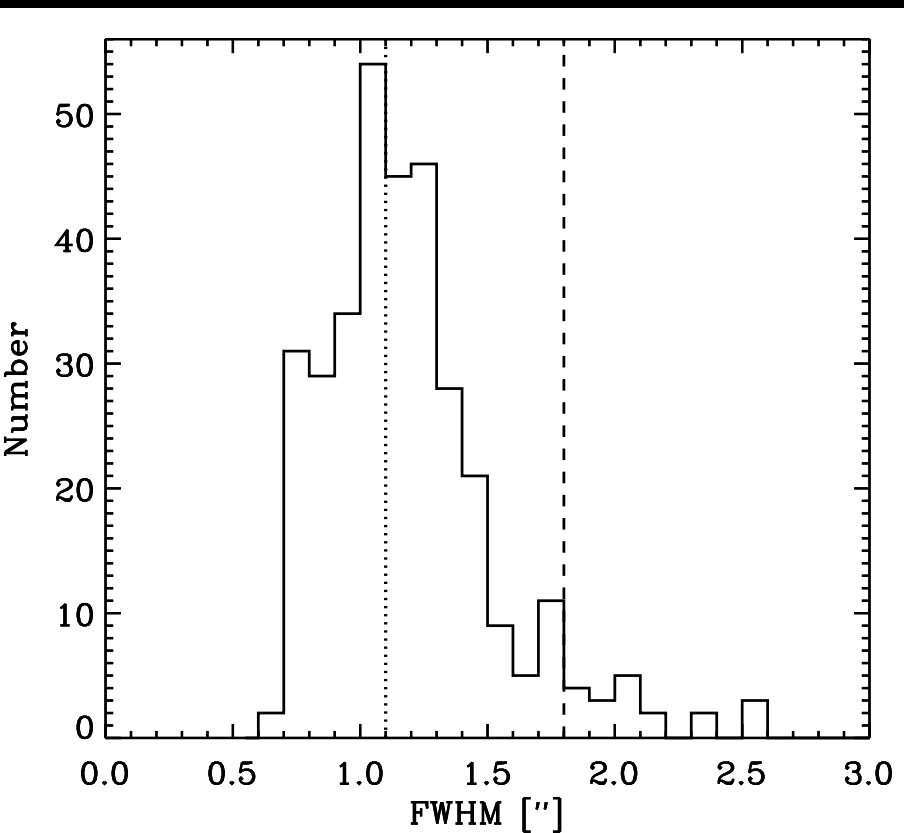
[RIGHT]: 8-epoch GO-Community extension in JWST Cycle $\gtrsim 1$.

NEP $2.0\mu m$ sky *always* dark: 0.24 ± 0.03 MJy/sr (GOODS $\simeq 0.19 - 0.35$).

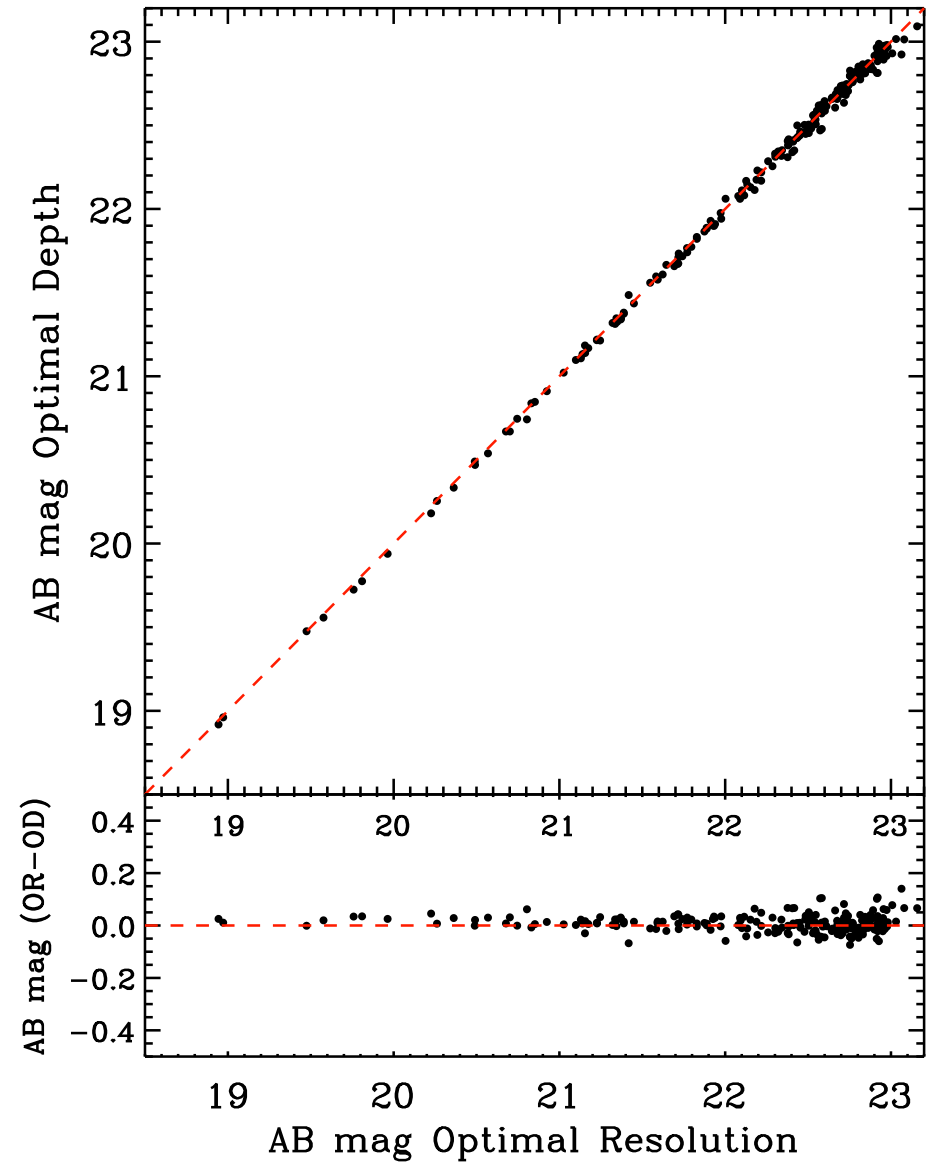
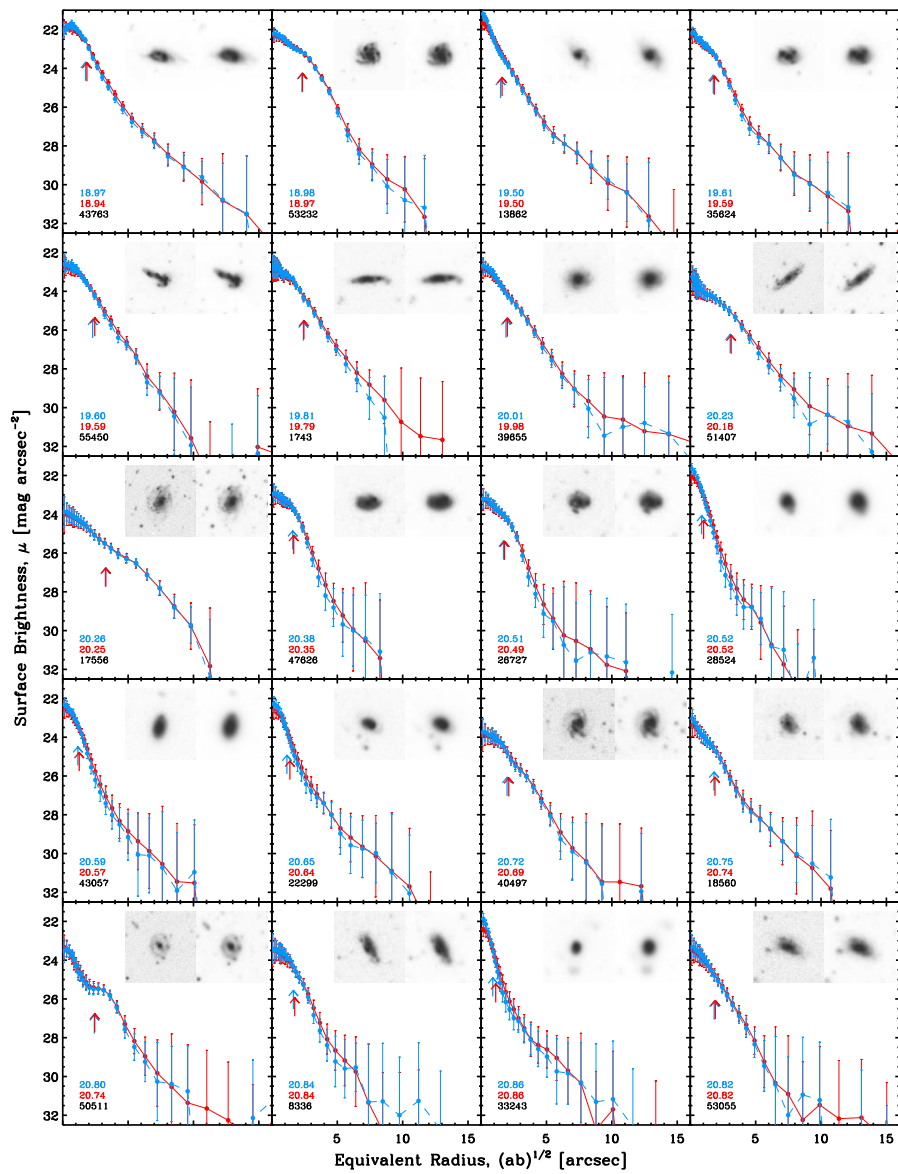
• NEP: time-domain imaging to $AB \lesssim 29$ & grism spectra to $AB \lesssim 28$ mag.



- Ashcraft⁺ (2018, PASP, 130, 064102): Seeing-sorted LBT U-band images:
- Optimal resolution image best for panchromatic SEDs of isolated objects
 - 30-hr Optimal depth U-band image goes deeper than HST UV images.

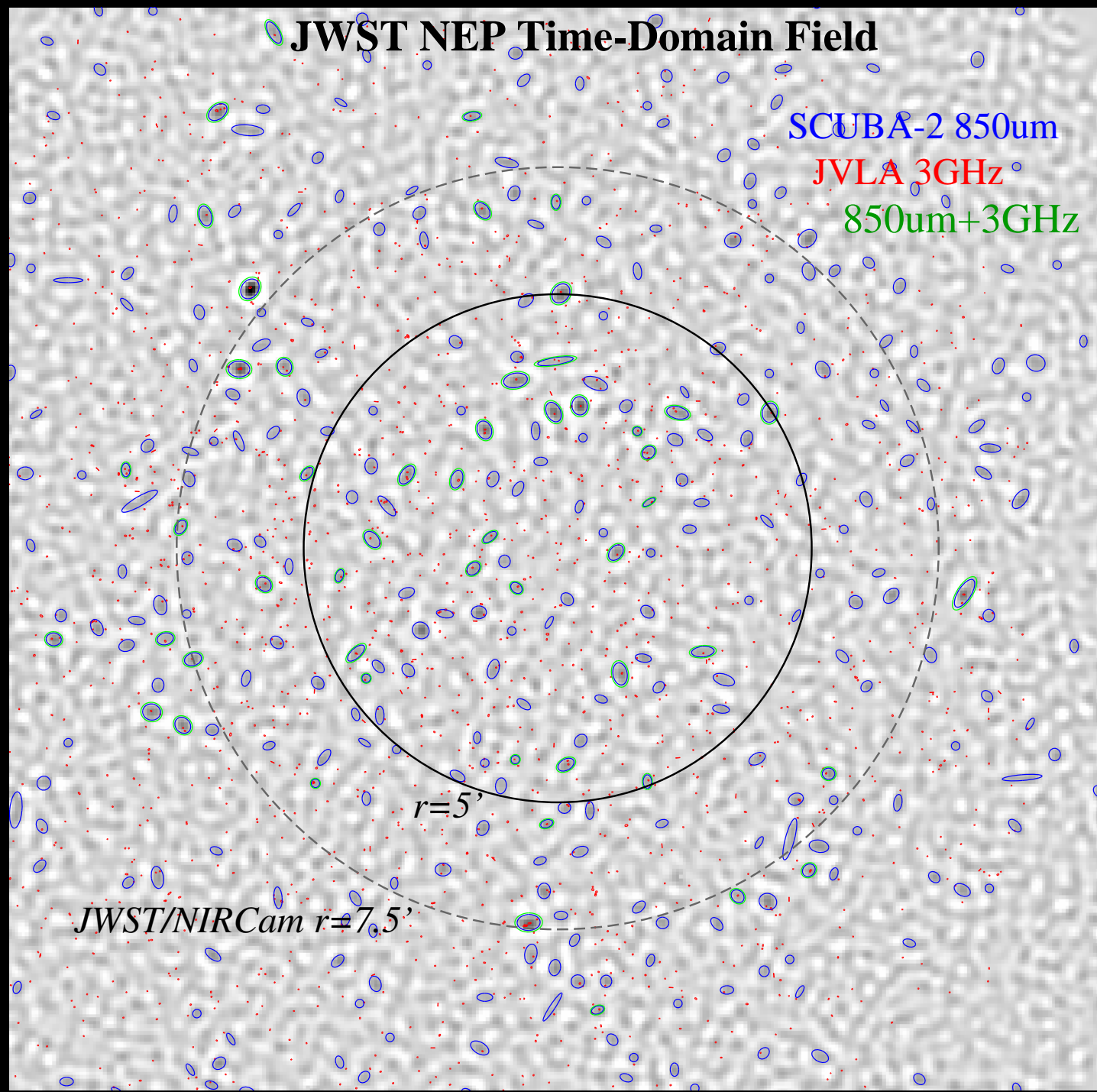


- 30-hr best-depth image (FWHM $\lesssim 1''.8$) reaches AB $\lesssim 28$ mag.
- 3-hr best-resolution image (FWHM $\lesssim 0''.8$) reaches AB $\lesssim 27$ mag, and is best for comparison to crowded HST UV and JWST IR images.
- Will have these from LBT and VLT in 2021 for NEP TDF and CANDELS.

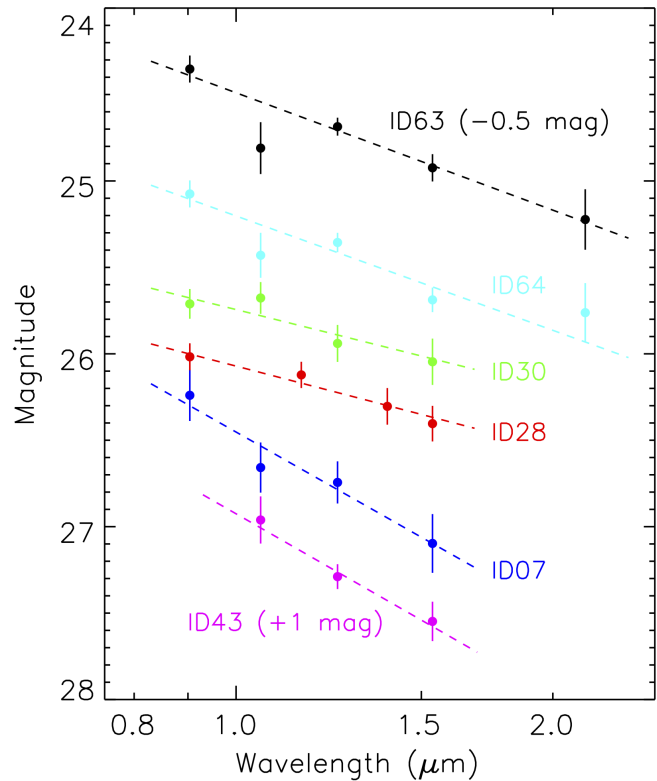


225 galaxies with $AB \simeq 19-23$ mag: light-profiles to $U \lesssim 32$ mag arcsec $^{-2}$ of best-res and best-depth images similar to $\lesssim 0.05-0.10$ mag.

→ No significant light missing in outskirts of galaxies that produce most EBL.



15-m JCMT SCUBA2 850 μ m map + VLA A+B-conf 3.0 GHz map
(~ 2500 sources to 4.5 μ Jy): trace cosmic SF incl. hidden SF & AGN.



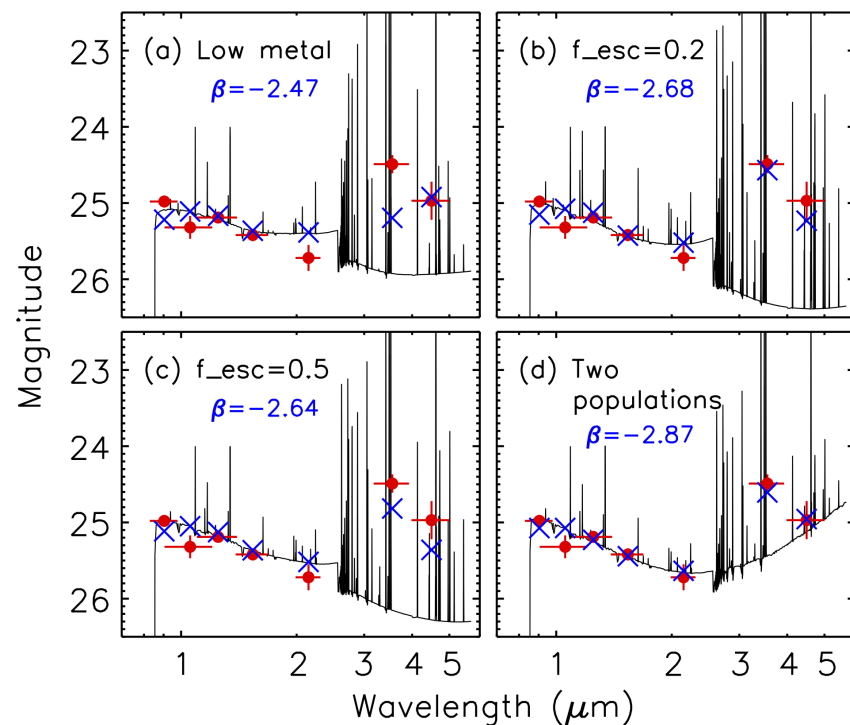
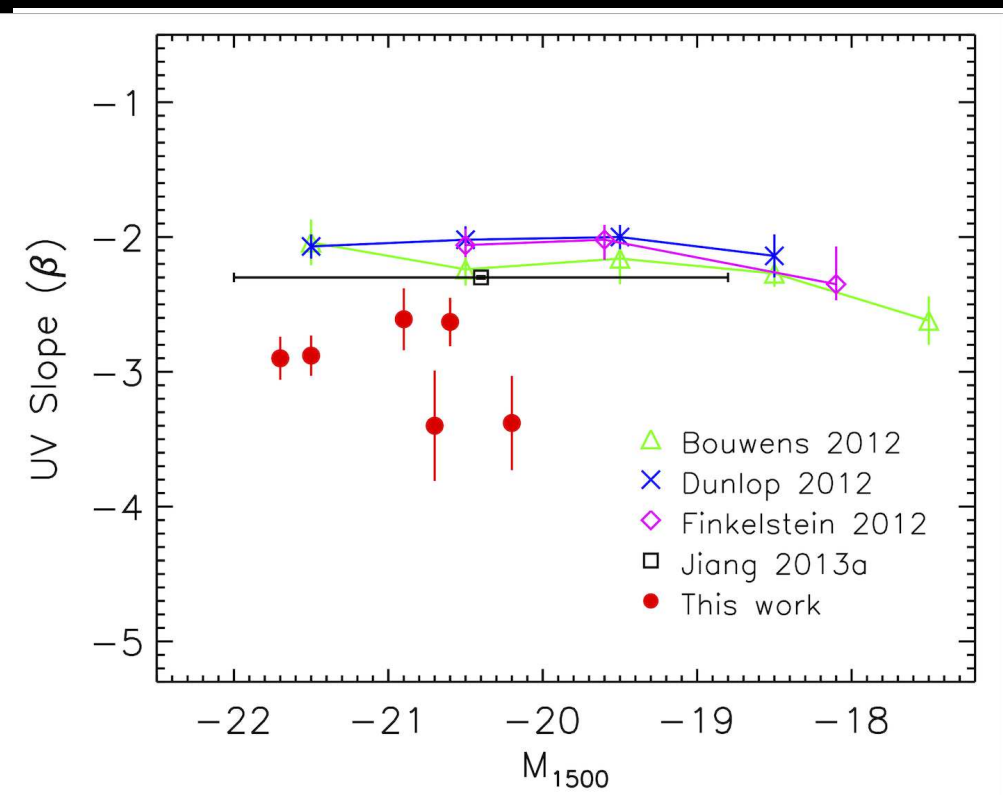
- L. Jiang et al. (2019): L^* galaxies at $z \simeq 6$ with extremely blue UV-SED β -slopes.

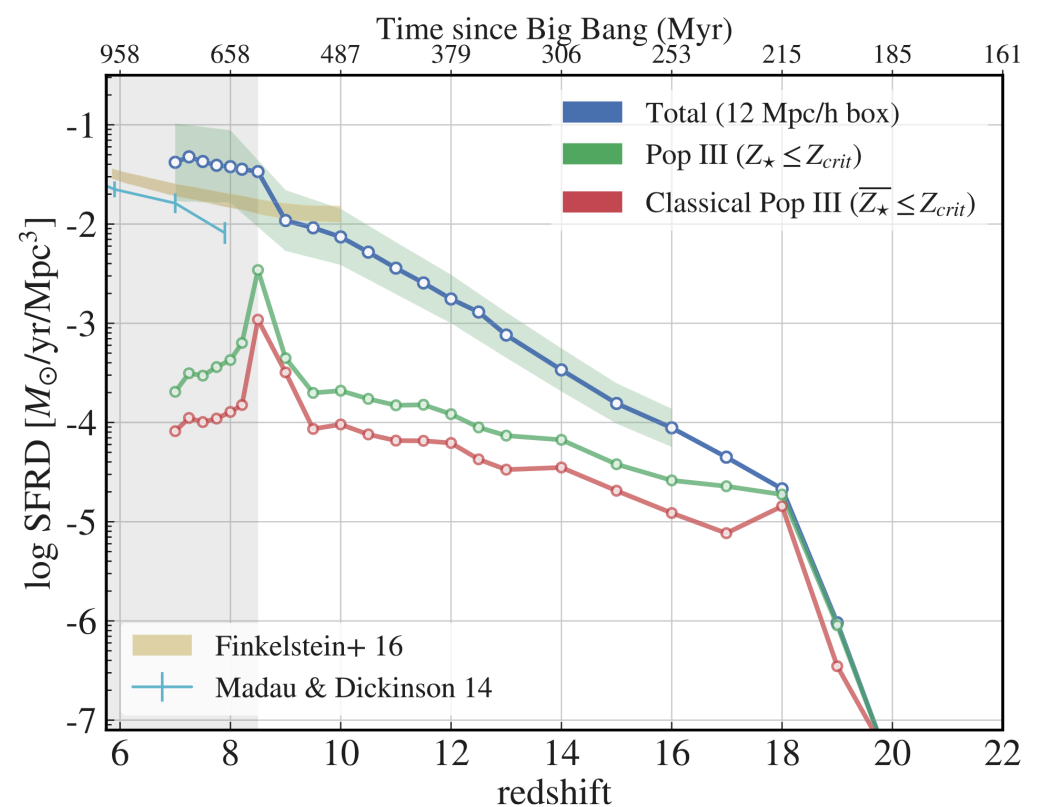
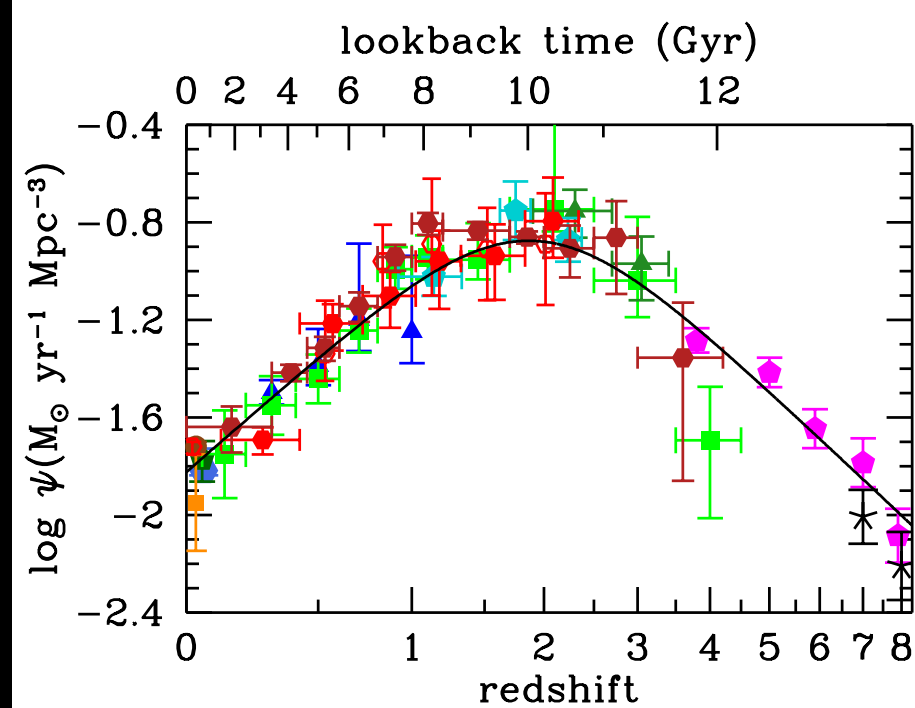
- Selected from 100's $z \simeq 6$ galaxies with Subaru, LBT, MMT images and solid Ly α spectra.

- HST WFC3-IR follow-up to precisely measure their UV β -slopes.

- Rare steep $\beta \simeq 2.4-2.9$ values requires either 2-component SED, or possibly some Pop III SED.

- Compelling targets for JWST NIRSpec, NIRCам.





Anticipated cosmic star-formation rate (SFR) at $z \gtrsim 7$:

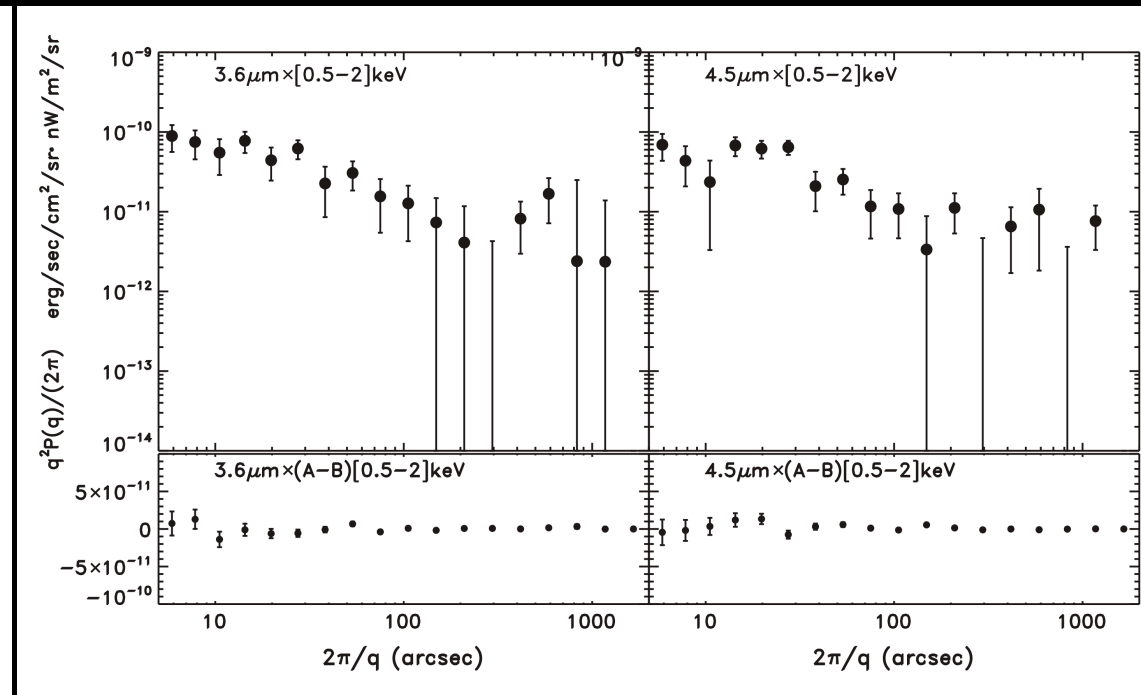
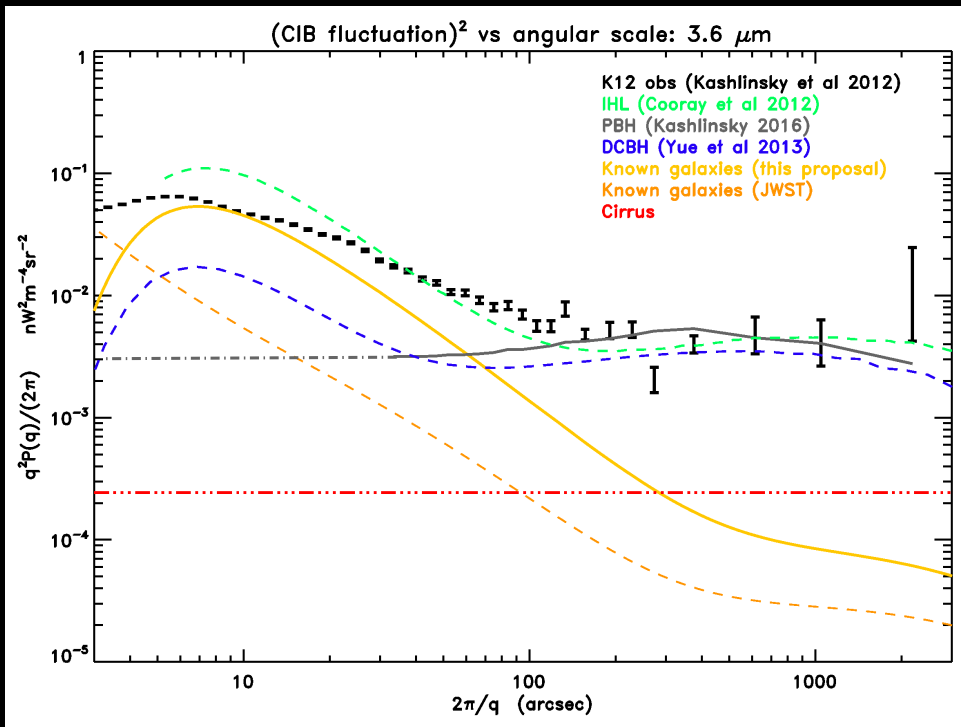
[LEFT] Observed SFH (Madau & Dickinson; 2014 ARAA, 52, 415);

[RIGHT] RAMSES models (*e.g.*, Sarmiento et al. 2018, ApJ, 854 75).

\Rightarrow Adopt this SFR from $z \simeq 17$ to $z \simeq 7$, implying at the lowest masses:

- Metallicity increases from ~ 0 at $z \simeq 18$ to $\lesssim 10^{-3}$ solar at $z \simeq 7$.
- Integrated SFR from $z \gtrsim 7$ has sky-SB $\gtrsim 31$ K-mag/arcsec $^{-2}$ (Windhorst et al. 2018), similar to the $3.6 \mu\text{m}$ CIB sky-SB possibly from BH's.

(3a) Limits to Pop III Sky-SB: First (Stellar-Mass?) Black Holes

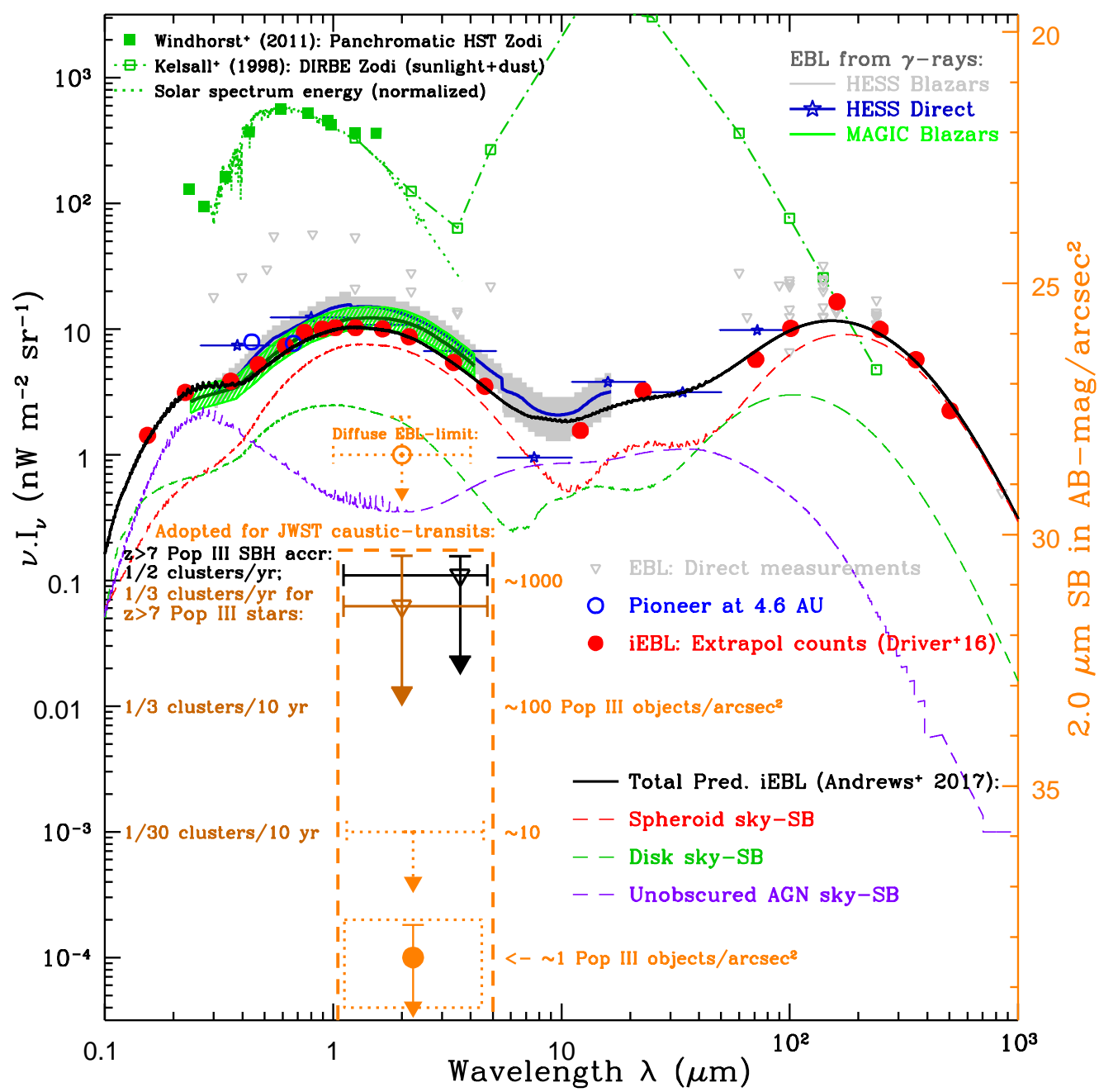


[LEFT] Object-free Spitzer 3.6 μm power-spectrum constrains noise fluctuation models (Cappelluti et al. 2017; Kashlinsky et al. 2012, 2015, 2018):

Explainable by: Primordial black hole or Direct-collapse black hole models.

[RIGHT] Spitzer–Chandra cross-corr spectrum (Mitchell-Wynne et al. 2016):

- $z \gtrsim 7$ objects have sky-SB fainter than 31 mag/arcsec², plus likely a (stellar mass) black hole X-ray component. (Kashlinsky⁺ 2018; Windhorst⁺ 2018, ApJ, 234, 41).



Extragalactic Background Light (Driver⁺ 16; Windhorst⁺ 18):

Energy(dust) \simeq 52% & energy(cosmic SF) \simeq 48% of EBL \Rightarrow dust wins!

Diffuse 1–4 μm sky \lesssim 0.1 nW/m²/sr or SB(K) \gtrsim 31 mag/arcsec²:

- 1) possibly from Pop III stars at $z \simeq 7-17$, and/or
- 2) their stellar-mass BH accretion disks ($z \simeq 7-8$).

This can make Pop III stars or their BH accretion disks temporarily visible to JWST & ground-based 30 meter telescopes at AB \lesssim 28–29 mag.

- Requires using the best lensing clusters and monitoring caustic transits.

(4) Possible caustic transits from Pop III stars and their BH accretion disks.



On the Observability of Individual Population III Stars and Their Stellar-mass Black Hole Accretion Disks through Cluster Caustic Transits

Rogier A. Windhorst¹, F. X. Timmes¹, J. Stuart B. Wyithe², Mehmet Alpaslan³, Stephen K. Andrews⁴, Daniel Coe⁵, Jose M. Diego⁶, Mark Dijkstra⁷, Simon P. Driver⁴, Patrick L. Kelly⁸, and Duho Kim¹

¹ School of Earth and Space Exploration, Arizona State University, Tempe, AZ 85287-1404, USA; Rogier.Windhorst@asu.edu, Francis.Timmes@asu.edu

² University of Melbourne, Parkville, VIC 3010, Australia; SWyithe@physics.unimelb.edu.au

³ New York University, Department of Physics, 726 Broadway, Room 1005, New York, NY 10003, USA

⁴ The University of Western Australia, 35 Stirling Highway, Crawley, WA 6009, Australia

⁵ Space Telescope Science Institute, 3700 San Martin Drive, Baltimore, MD 21218, USA

⁶ IFCA, Instituto de Fisica de Cantabria (UC-CSIC), Avenida de Los Castros s/n, E-39005 Santander, Spain

⁷ Institute of Theoretical Astrophysics, University of Oslo, NO-0315 Oslo, Norway

⁸ University of California at Berkeley, Berkeley, CA 94720-3411, USA

Received 2017 November 22; revised 2018 January 6; accepted 2018 January 10; published 2018 February 14

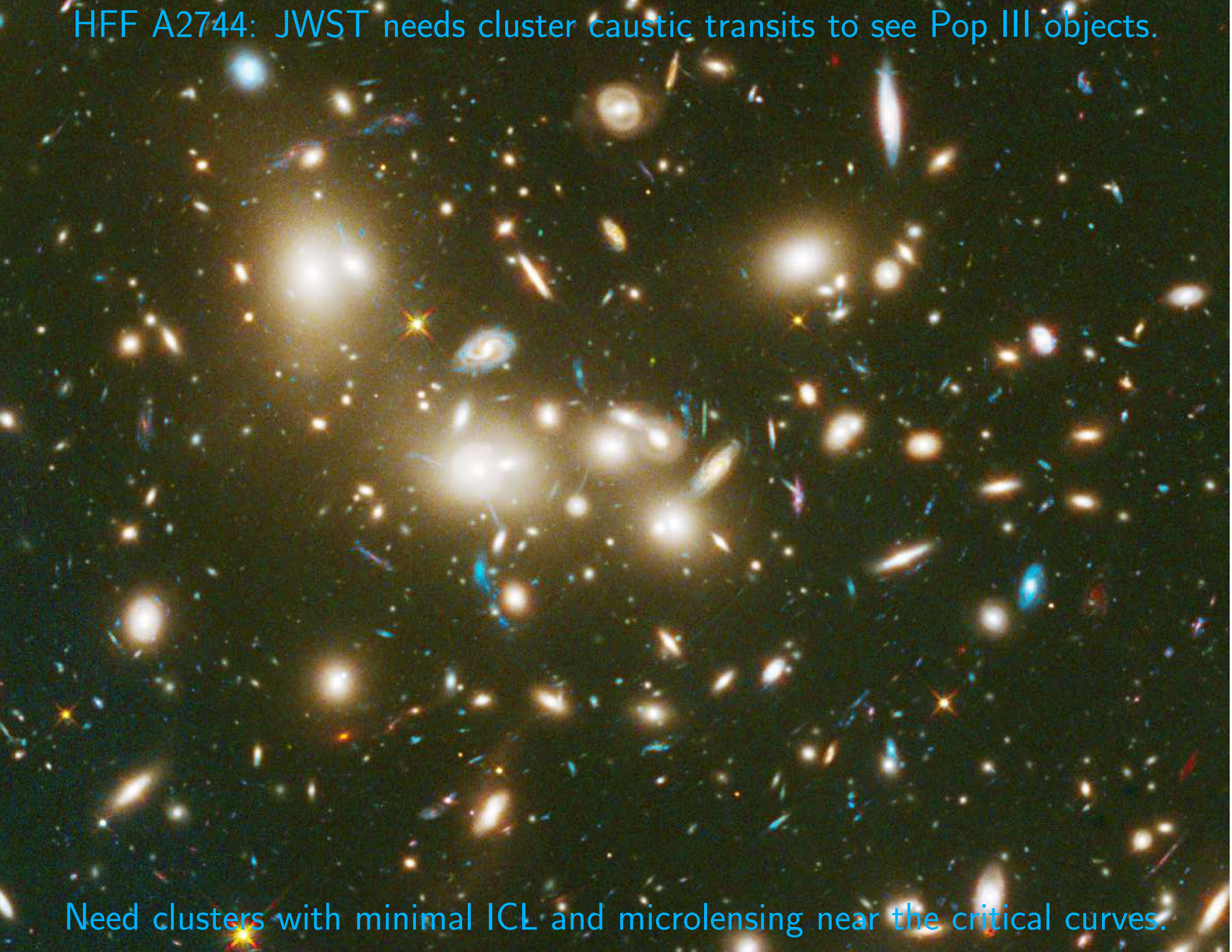
Abstract

We summarize panchromatic Extragalactic Background Light data to place upper limits on the integrated near-infrared surface brightness (SB) that may come from Population III stars and possible accretion disks around their stellar-mass black holes (BHs) in the epoch of First Light, broadly taken from $z \simeq 7$ –17. Theoretical predictions and recent near-infrared power spectra provide tighter constraints on their sky signal. We outline the physical properties of zero-metallicity Population III stars from MESA stellar evolution models through helium depletion and of BH accretion disks at $z \gtrsim 7$. We assume that second-generation non-zero-metallicity stars can form at higher multiplicity, so that BH accretion disks may be fed by Roche-lobe overflow from lower-mass companions. We use these near-infrared SB constraints to calculate the number of caustic transits behind lensing clusters that the *James Webb Space Telescope* and the next-generation ground-based telescopes may observe for both Population III stars and their BH accretion disks. Typical caustic magnifications can be $\mu \simeq 10^4$ – 10^5 , with rise times of hours and decline times of $\lesssim 1$ year for cluster transverse velocities of $v_T \lesssim 1000$ km s⁻¹. Microlensing by intracluster-medium objects can modify transit magnifications but lengthen visibility times. Depending on BH masses, accretion-disk radii, and feeding efficiencies, stellar-mass BH accretion-disk caustic transits could outnumber those from Population III stars. To observe Population III caustic transits directly may require monitoring 3–30 lensing clusters to AB $\lesssim 29$ mag over a decade.

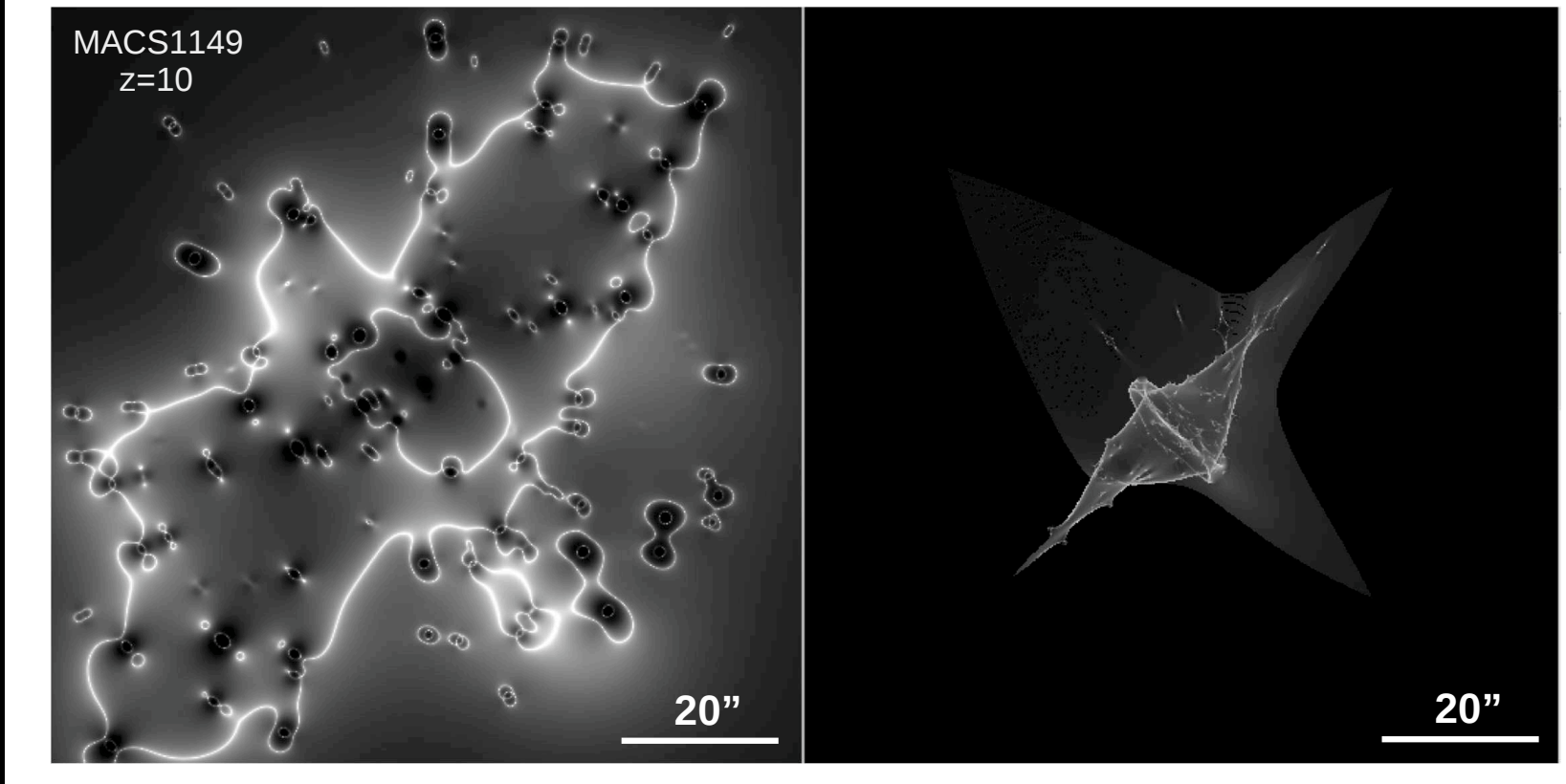
Key words: accretion, accretion disks – galaxies: clusters: general – gravitational lensing: strong – infrared: diffuse background – stars: black holes – stars: Population III

- JWST (and ground-based 25–39 m telescopes) may detect Pop III stars and their stellar-mass BH accretion disks *directly* to AB $\lesssim 28$ –29 mag via cluster caustic transits (Windhorst⁺, 2018, ApJS, 234, 41).
- JWST GO community should anticipate this and build on it.

HFF A2744: JWST needs cluster caustic transits to see Pop III objects.



Need clusters with minimal ICL and microlensing near the critical curves.



For source at $z=10$, critical curves for HFF cluster MACS 1149 at $z \simeq 0.54$ [LEFT], and main cluster caustics [in the source plane; RIGHT].

- Transverse cluster (sub-component) velocities can be $v_T \lesssim 1000$ km/s (Kelly⁺ 2018; Nature Astr. 2, 334; Windhorst⁺ 2018, ApJS, 234, 41).
- Main caustic magnification: $\mu \simeq 10 \cdot (d_{caustic}/'')^{-1/2}$. For Pop III objects at $z \gtrsim 7$ with $1-30 R_{\odot}$, μ can be $\gtrsim 10^4 - 10^5$ for $\lesssim 0.4$ year.
- Must use clusters with minimal ICL near the critical curves, since ICL microlensing dilutes the main caustics (Diego⁺ 2018, ApJ, 857, 25).

(4) HST observations of a B-star caustic transit at $z \simeq 1.49$

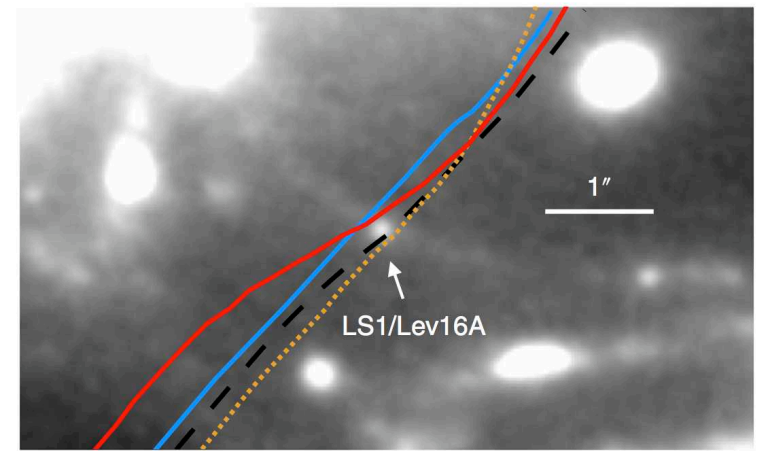
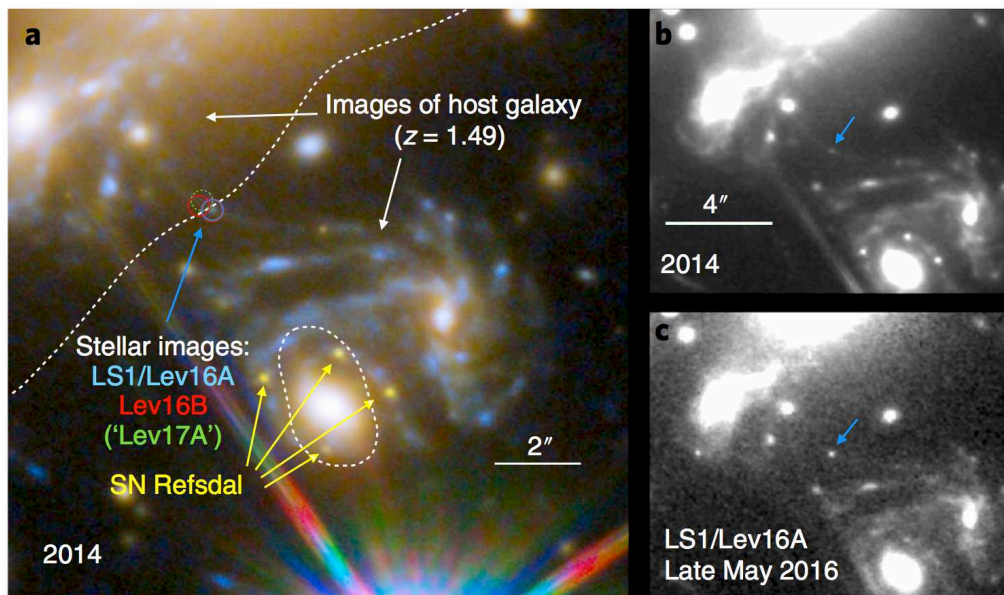


Fig. 2 | Proximity of LS1/Lev16A to the MACS J1149 galaxy cluster's critical curve for multiple galaxy-cluster lens models. Critical curves for models with available high-resolution lens maps including ref. ⁸ (CATS);

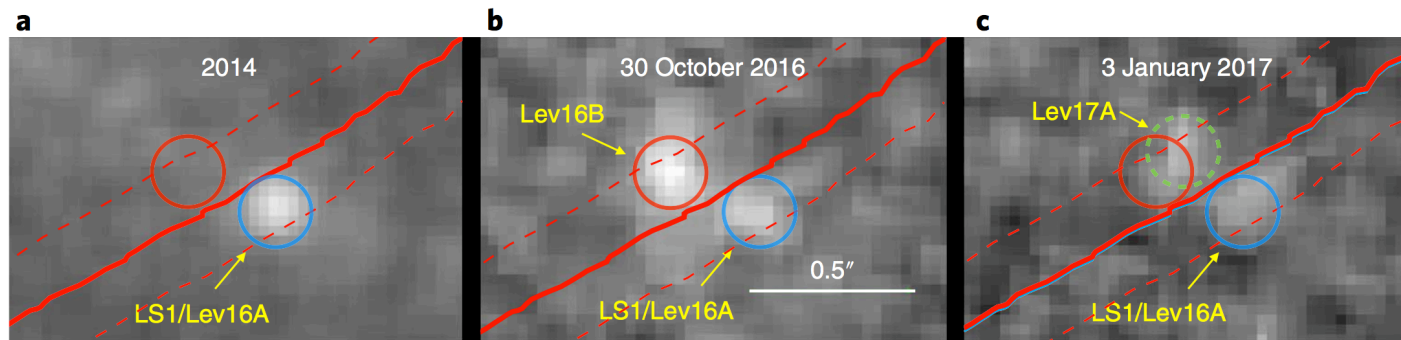


Fig. 5 | Highly magnified stellar images located near the MACS J1149 galaxy cluster's critical curve. **a**, LS1 in 2014; we detected LS1 when it temporarily brightened by a factor of ~ 4 in late April 2016, and its position is marked by a blue circle. **b**, The appearance of a new image dubbed Lev16B on 30 October 2016, whose position is marked by a red circle. The solid red line marks the location of the cluster's critical curve from the CATS cluster model⁸, and the dashed red lines show the approximate 1σ uncertainty from comparison of multiple cluster lens models⁵⁻¹⁰. Lev16B's position is consistent with the possibility that it is a counterimage of LS1. **c**, The candidate named Lev17A at the location of the green dashed circle had a $\sim 4\sigma$ significance detection on 3 January 2017. If a microlensing peak, Lev17A must correspond to a different star.

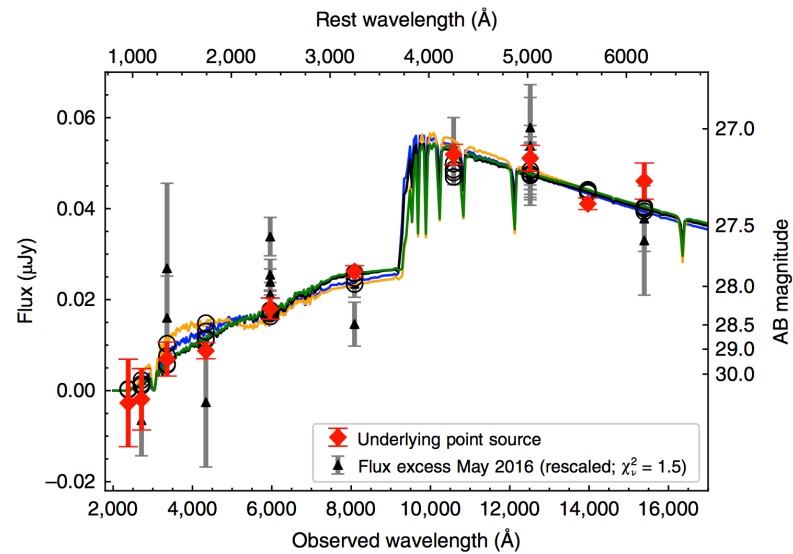
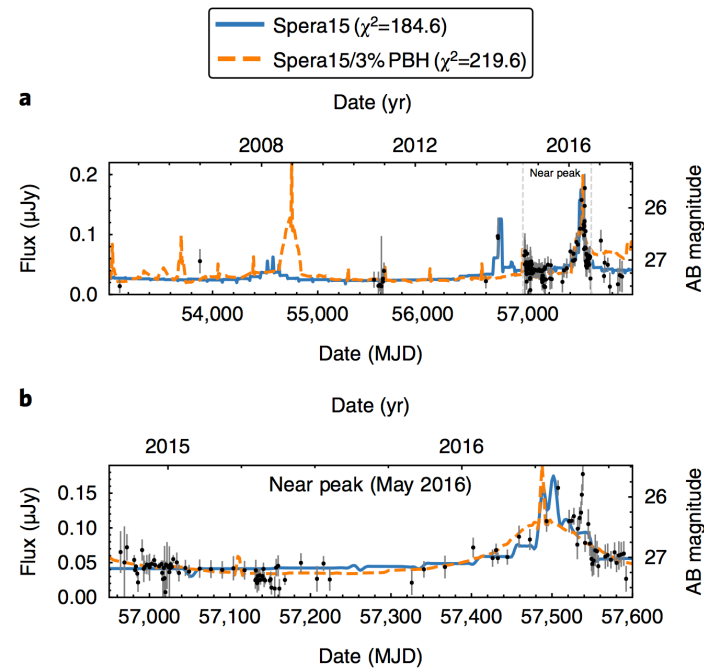


Fig. 3 | The SEDs of LS1 measured in 2013–2015 and of the rescaled excess flux density at LS1’s position close to its May 2016 peak. Rescaling the SED of the flux excess (Lev16A; black triangles) to match that of the



Kelley et al. 2018 (Nat. Astr. 2, 334): caustic transit of a B-star at $z \approx 1.49$.

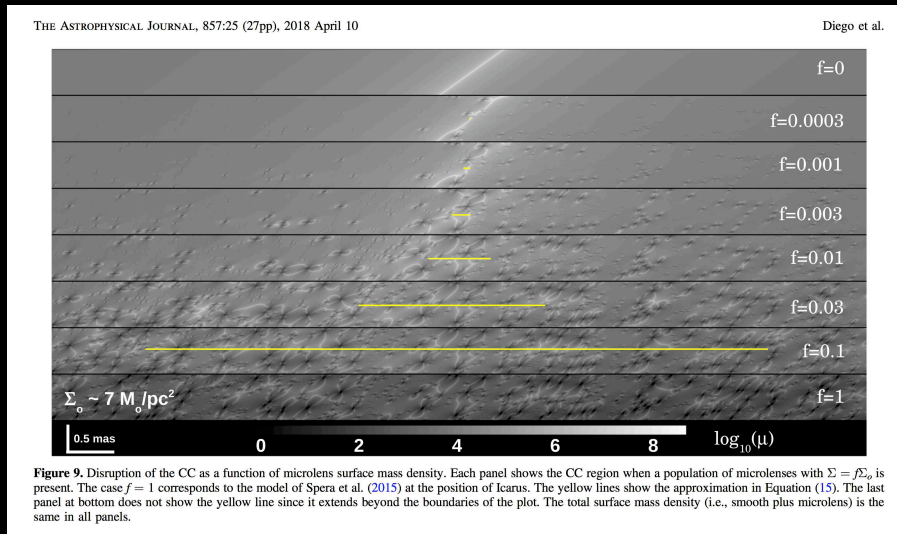
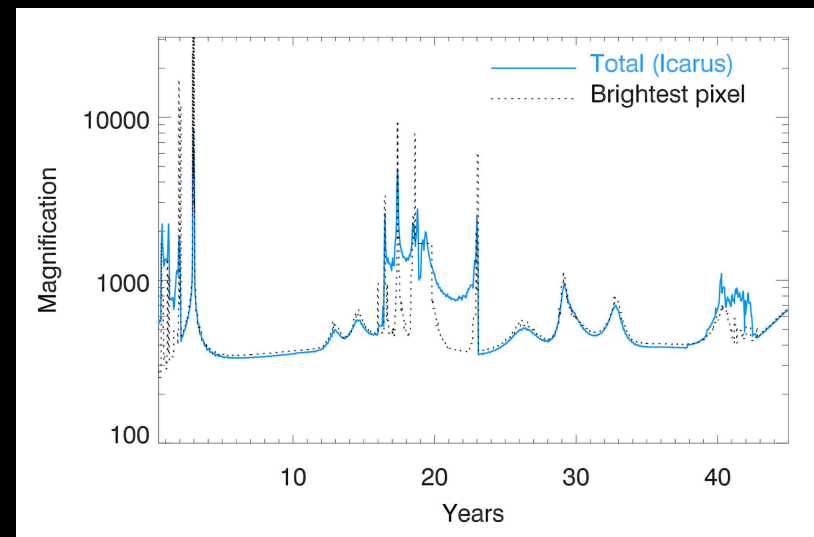
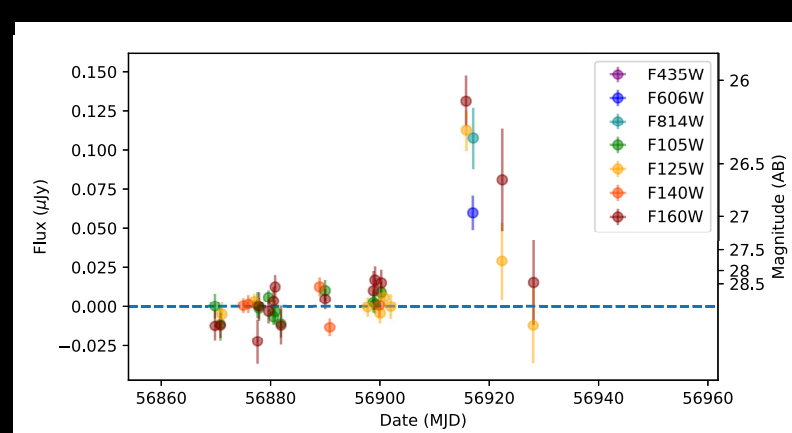
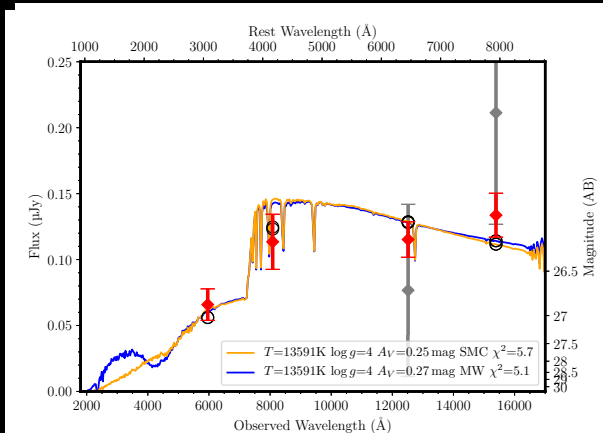
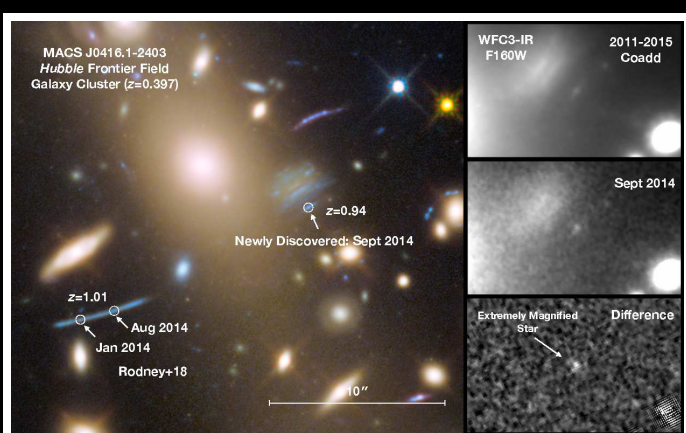
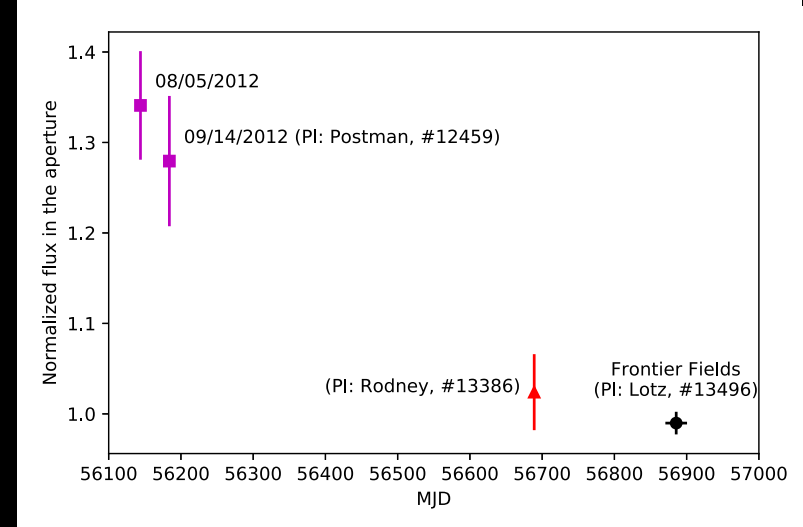
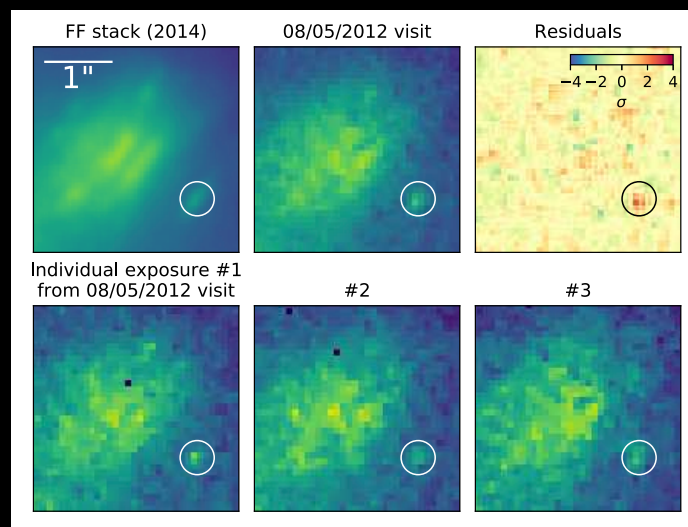
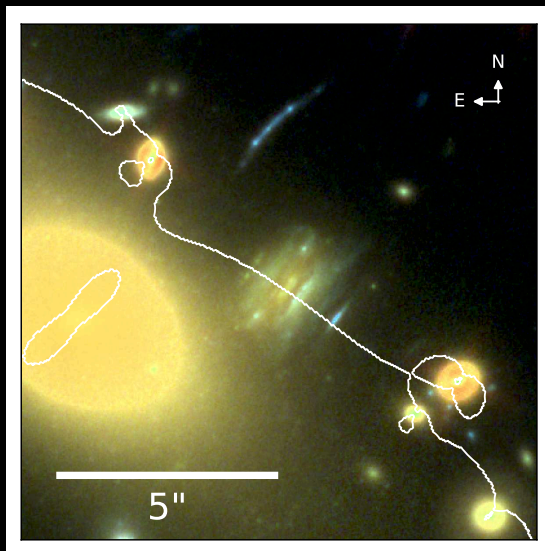


Figure 9. Disruption of the CC as a function of microlens surface mass density. Each panel shows the CC region when a population of microlenses with $\Sigma = f\Sigma_0$ is present. The case $f = 1$ corresponds to the model of Spera et al. (2015) at the position of Icarus. The yellow lines show the approximation in Equation (15). The last panel at bottom does not show the yellow line since it extends beyond the boundaries of the plot. The total surface mass density (i.e., smooth plus microlens) is the same in all panels.



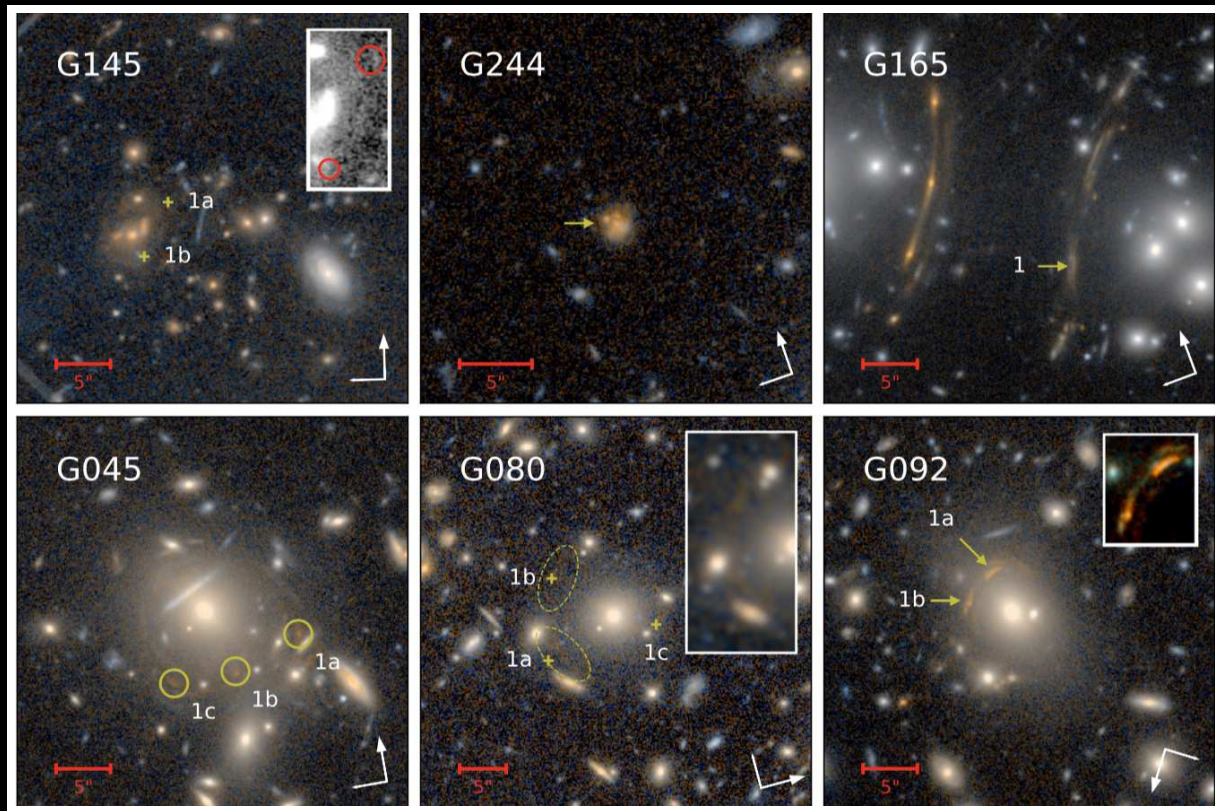
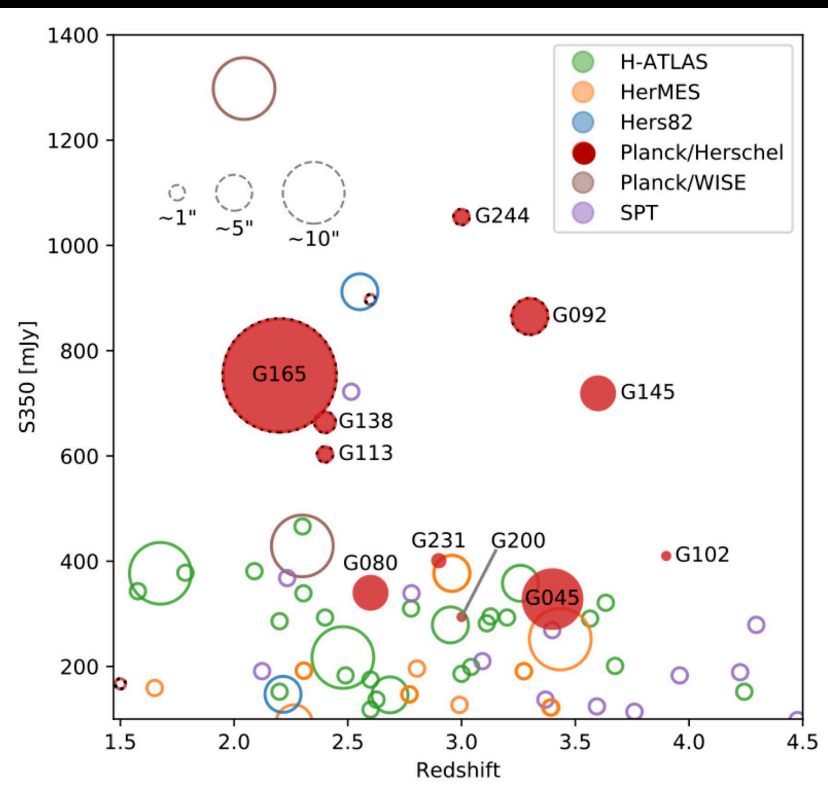
Diego⁺ 2018 (ApJ, 857, 25): caustic transits in the presence of microlensing. See also Miralda-Escudé (1991), Venumadhav et al. (2017, ApJ, 850, 49).



(Top) Caustic Transit at $z \simeq 0.94$ by Kaurov et al. (2019, ApJ, 880, 58)

(Bottom) Caustic Transits at $z \sim 1$ by Chen et al. (2019, ApJ, 881, 8)

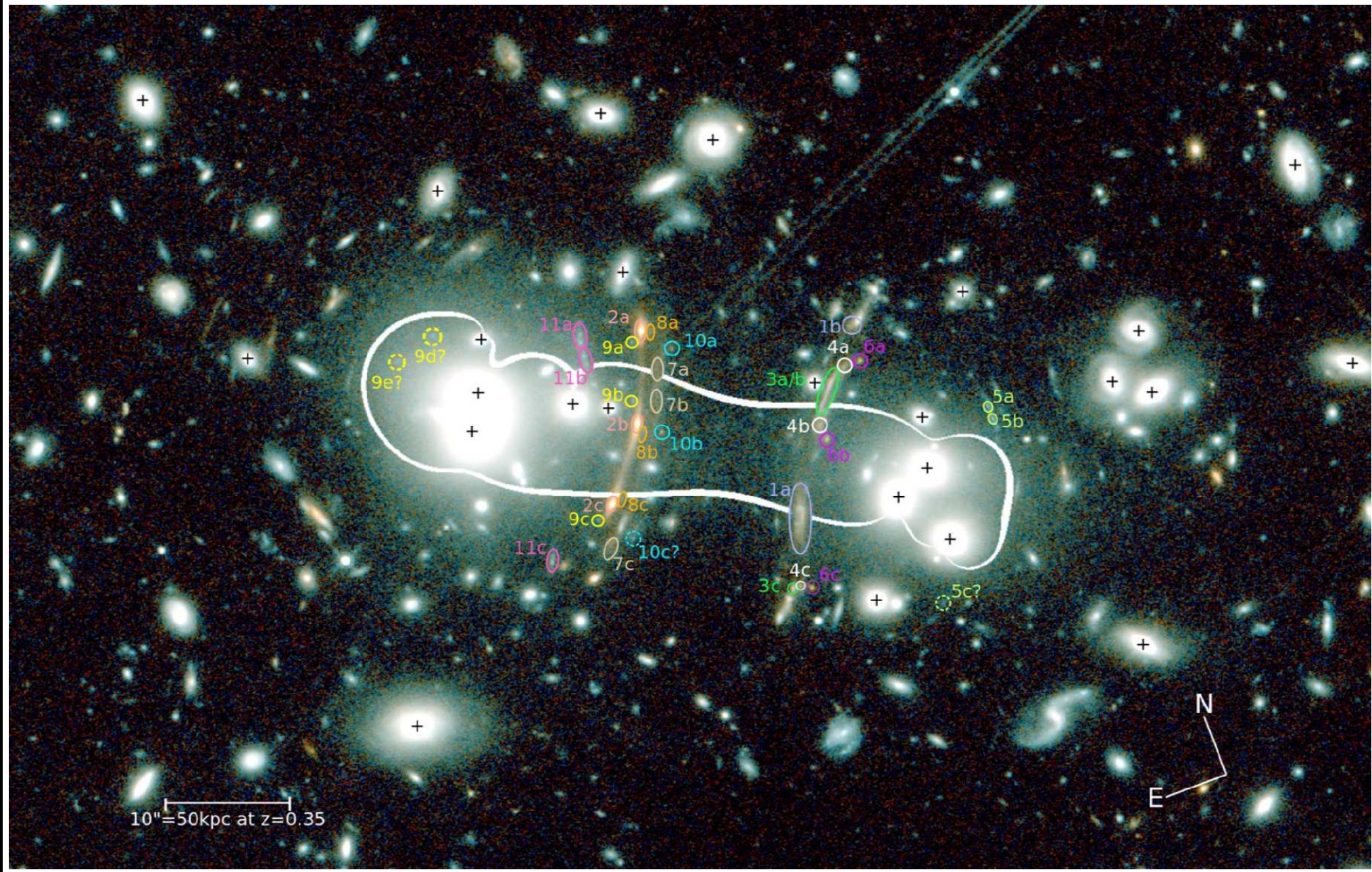
- A $T \simeq 13,500$ B giant at $z \simeq 0.94$ with magnification $\mu \gtrsim 200-300$.
- MACS 0416 ICL microlensing complicates analysis (at lower z 's).



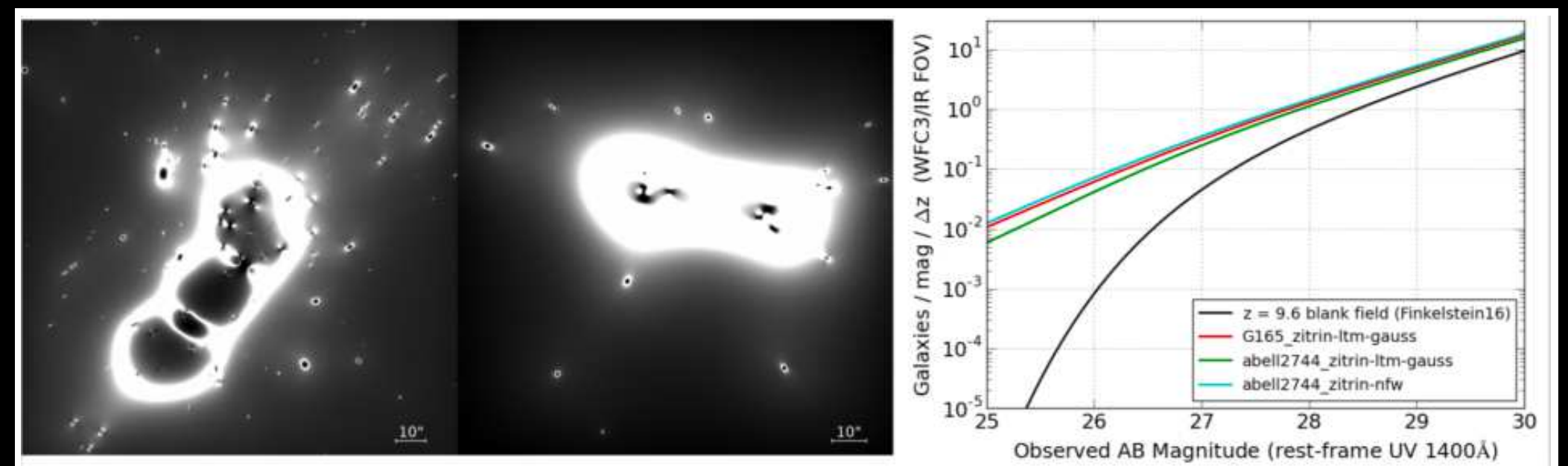
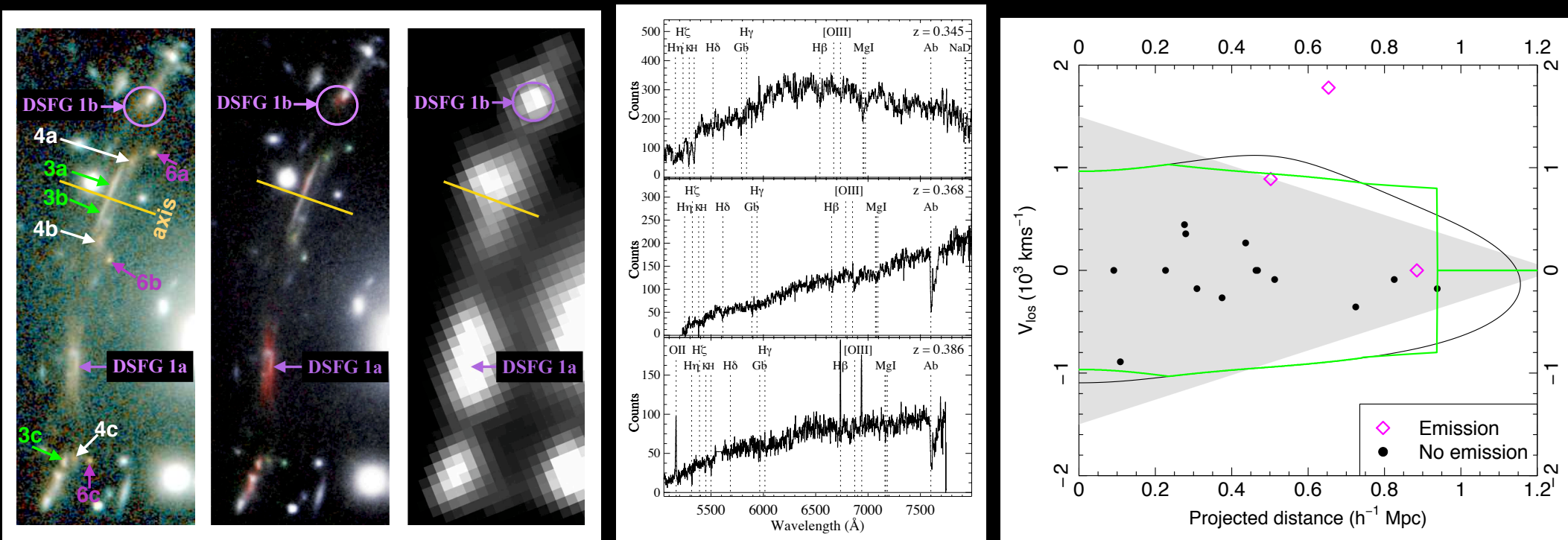
[Left] Herschel/Planck selected clusters with highly lensed $350 \mu\text{m}$ sources (Frye et al. 2019, ApJ, 781, 51):

[Right] G165 at $z \simeq 0.35$ is one of the brightest *and* most massive ($M \simeq 1.9 \times 10^{15} M_{\odot}$) Planck selected clusters.

- Its high S_{350} flux of ~ 750 mJy is due to a strongly lensed dusty star-forming galaxy (DSFG) at $z \simeq 2.2$.
- G165 may be as good as A 2744 in magnifying First Light sources, and as good as M0416 for caustic transits.

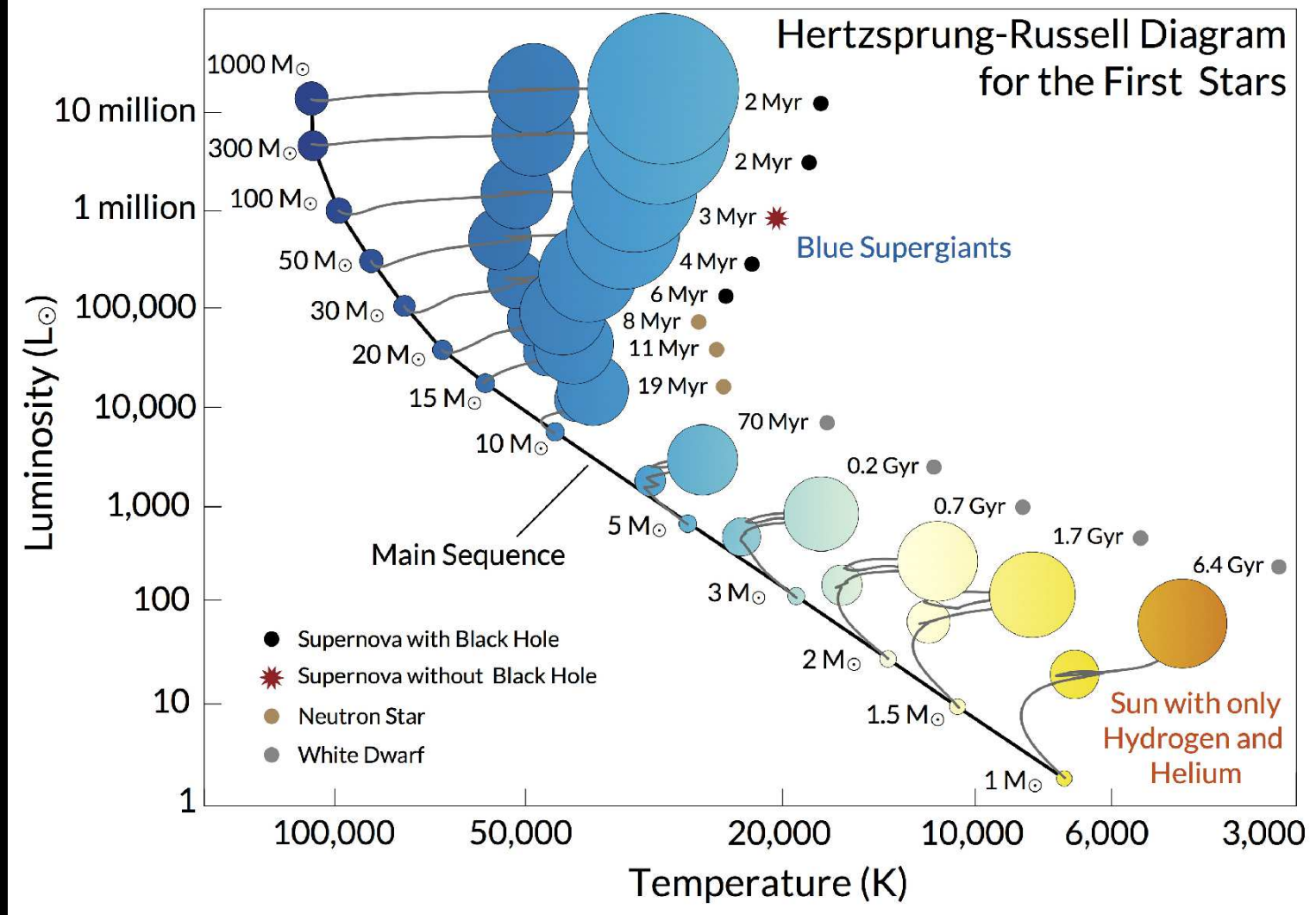


- G165 has two giant lensed arcs at $z \simeq 2.2$, and 11 lensed image families.
- Very prominent cluster substructure. Combined with its MMT N ($z \simeq 0.35$), suggests significant transverse velocity needed for caustic transits.



[Top] WFC3 JH, LBT K; MMT spectra; "Trumpet" diagram for G165.

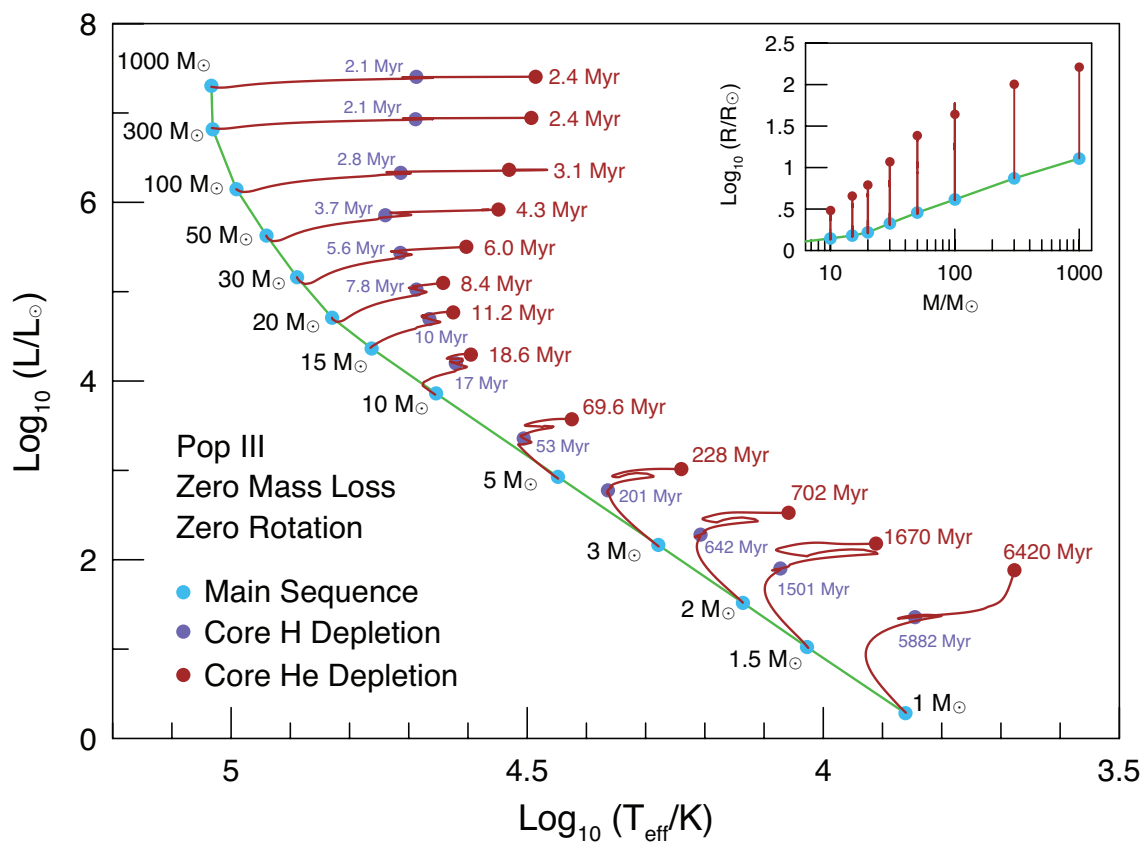
[Bottom] Magnification maps G165 & A2744; Lensing bias for $z \simeq 10$ LF.



Pop III star HR-diagram: MESA stellar evolution models for $z=0.0$ Z_{\odot} .

(Windhorst, Timmes, Wyithe et al. 2018, ApJS, 234, 41):

- Critical point: 30–1000 M_{\odot} Pop III stars ($Z=0.00$ Z_{\odot}) live $\sim 10\times$ shorter than 2–5 M_{\odot} Pop III stars in their AGB stage.
- Hence, 2–5 M_{\odot} AGB companion stars can feed the LIGO-mass BHs left over from $M \gtrsim 30$ M_{\odot} Pop III stars (assuming binaries in 2nd generation).



Windhorst⁺ (2018, ApJS, 234, 41):

- Multicolor accretion-disk models for stellar-mass black holes [RIGHT]: For $M_{BH} \simeq 5\text{--}700 M_{\odot}$, accretion disk radii and luminosities are similar to those of Pop III AGB stars, when the BH is fed by a Roche lobe-filling lower-mass companion star on the AGB (which live $\gtrsim 10\times$ longer!).
- Assumes 2nd generation O-stars have high enough Fe/H ($\gtrsim 10^{-4} Z_{\odot}$) that $2\text{--}5 M_{\odot}$ AGB companion stars exist and feed these LIGO-mass BHs.
- This may make stellar-mass black hole accretion disks at least as likely to be seen via caustic transits as the Pop III stars themselves.

Table 2. Implied ZAMS Pop III Star Observational Parameters Relevant to Caustic Transit Calculations

Mass ^a ZAMS (M_{\odot})	T_{eff}^b (K)	Radius ^c — at ZAMS — (R_{\odot})	L_{bol}^d (L_{\odot})	M_{bol}^e (AB)	Bolo+IGM+K-corr ^f			ZAMS m_{UV}^g			t_{rise}^h (hr)	transit ⁱ rate (/cl/yr)
					z=7	z=12	z=17	z=7	z=12	z=17		
1.0	7.266e3	0.87	1.92	+4.03	+4.44	+3.13	+2.61	57.71	57.74	58.07	0.17	8×10^5
1.5	1.065e4	0.95	10.5	+2.18	+1.45	+0.42	-0.06	52.87	53.18	53.55	0.18	1.1×10^4
2.0	1.367e4	1.03	32.9	+0.95	+0.30	-0.59	-1.06	50.49	50.93	51.31	0.20	1.5×10^3
3.0	1.899e4	1.12	146.	-0.67	-0.51	-1.26	-1.72	48.06	48.64	49.03	0.22	182.
5.0	2.805e4	1.23	846.	-2.58	-0.70	-1.35	-1.80	45.96	46.65	47.04	0.24	29.1
10	4.508e4	1.40	7.28e3	-4.91	-0.22	-0.79	-1.23	44.10	44.88	45.27	0.27	5.70
15	5.789e4	1.51	2.32e4	-6.17	+0.23	-0.30	-0.75	43.30	44.10	44.50	0.29	2.78
20	6.754e4	1.65	5.11e4	-7.03	+0.56	+0.04	-0.40	42.77	43.59	43.99	0.32	1.74
30	7.737e4	2.12	1.45e5	-8.16	+0.88	+0.36	-0.08	41.95	42.78	43.17	0.41?	0.82?
50	8.713e4	2.86	4.25e5	-9.33	+1.17	+0.66	+0.22	41.08	41.91	42.31	0.55*	0.37*
100	9.796e4	4.12	1.40e6	-10.63	+1.47	+0.96	+0.52	40.08	40.91	41.31	0.80*	0.15*
300	1.074e5	7.41	6.56e6	-12.30	+1.71	+1.21	+0.77	38.64	39.48	39.88	1.43*	0.039*
1000	1.080e5	12.9	2.02e7	-13.52	+1.72	+1.22	+0.78	37.44	38.28	38.68	2.48*	0.013*

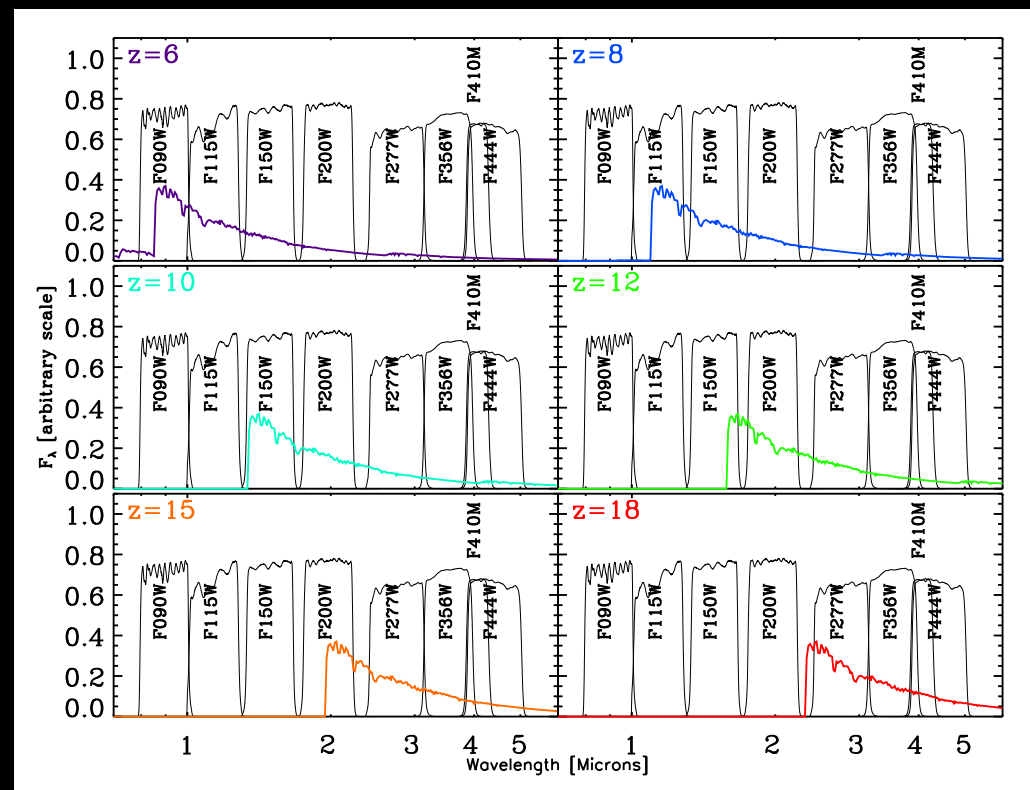
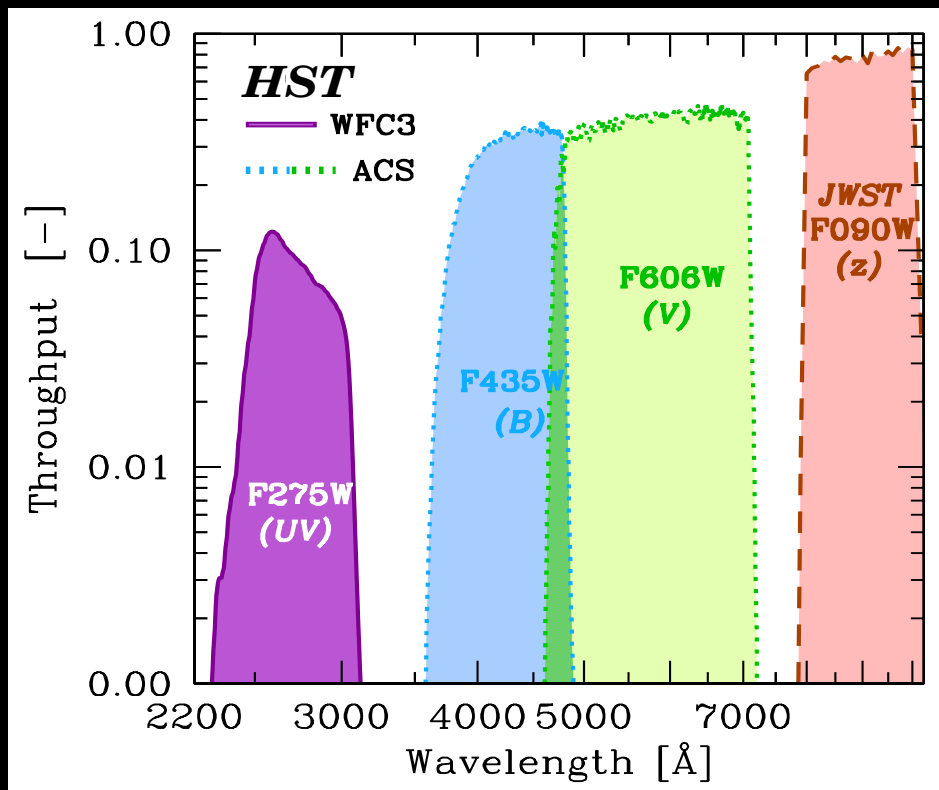
- If $M \gtrsim 30 M_{\odot}$ Pop III ZAMS stars have $\mu \gtrsim 10^4 - 10^5$ during caustic transits, they could be detectable for months to $AB \lesssim 29$ mag with JWST.
- Expect $\lesssim 1$ caustic transit/yr at $z \gtrsim 7$ when JWST monitors $\gtrsim 3$ clusters.

Conclusions

Panchromatic X-ray–Radio data accumulating for NEP Time-Domain Field.

- We are also getting the best possible (ground-based) data before JWST flies on some of the best lensing clusters.
- $M \gtrsim 30 M_{\odot}$ Pop III ZAMS stars ($AB \sim 37\text{--}42$ mag at $z \gtrsim 7$), with $\mu \gtrsim 10^4\text{--}10^5$ during caustic transits, detectable (for months) to $AB \lesssim 29$ with JWST.
- Pop III stellar mass black hole ($M \gtrsim 20 M_{\odot}$) accretion disks also be ~ 1 mag brighter *and* live $\sim 10\times$ longer than their ZAMS stars.
- JWST could detect *both* Pop III stars and their stellar-mass BH ($M \gtrsim 20 M_{\odot}$) accretion disks at $AB \lesssim 28\text{--}29$ mag via caustic transits for magnifications $\mu \simeq 10^4\text{--}10^5$ (where ICL microlensing doesn't dominate caustics).
- JWST GO community is anticipating this, and planning for it.

SPARE CHARTS

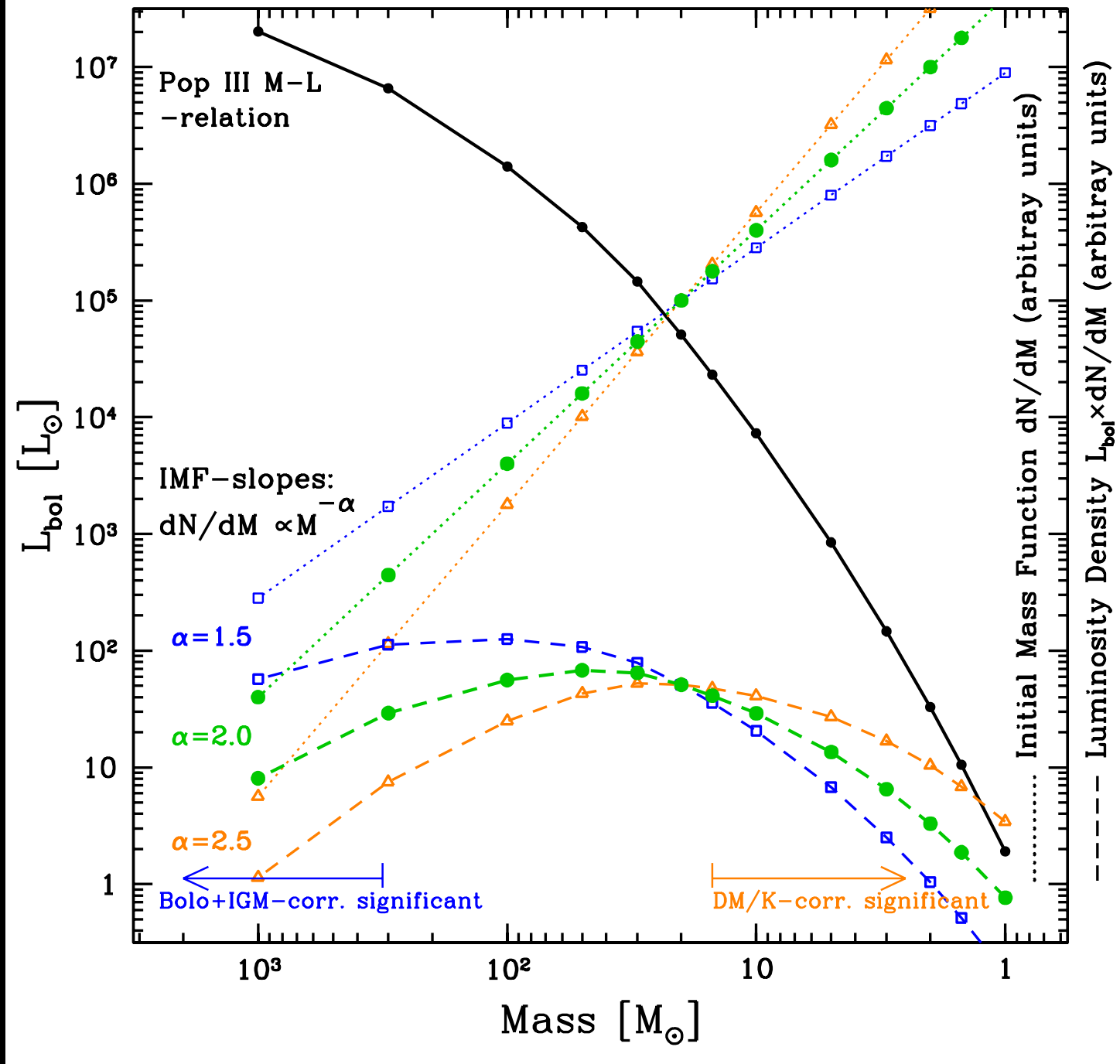


[LEFT] HST UV-vis filters complement the JWST NEP community field:

- HST adds λ 's inaccessible to JWST, or where HST has better PSF.

[RIGHT] Standard 8-band 0.8–5 μm filter set for JWST NIRCams.

- These are what GTO's will use as standard NIRCams filters.



Mass–Luminosity relation for zero metallicity Pop III MESA models:
 For range of IMF slopes, most Pop III star sky-SB comes from 20–300 M_{\odot} .

Table 1. Adopted Pop III Star Physical Parameters from MESA models^a

Mass (M_{\odot})	Age	T_{eff} (K)	log R (R_{\odot})	log L_{bol} (L_{\odot})	T_{eff} (K)	log R (R_{\odot})	log L_{bol} (L_{\odot})	Age	T_{eff} (K)	log R (R_{\odot})	log L_{bol} (L_{\odot})	Age	Time ^b (Myr)
	Pre-MS (Myr)							— at ZAMS —				— at Hydrogen-depletion —	
1.0	9.28	7.266e3	-0.0581	0.2825	6.999e3	0.5119	1.3576	5882	— ^c	—	—	6420	538
1.5	6.11	1.065e4	-0.0203	1.0227	1.181e4	0.3292	1.9015	1501	8.149e3	0.7913	2.1804	1670	169
2.0	3.02	1.367e4	0.0108	1.5177	1.611e4	0.2498	2.2815	642	1.145e4	0.6685	2.5249	702	60
3.0	1.38	1.899e4	0.0487	2.1654	2.311e4	0.1843	2.7770	201	1.736e4	0.5510	3.0138	228	27
5.0	0.56	2.805e4	0.0911	2.9274	3.206e4	0.1903	3.3581	53	2.658e4	0.4608	3.5732	70	17
10	0.23	4.508e4	0.1462	3.8618	4.174e4	0.3807	4.1972	17	3.938e4	0.4811	4.2968	19	1.6
15	0.13	5.789e4	0.1803	4.3647	4.624e4	0.5401	4.6937	10	4.215e4	0.6581	4.7691	11	0.8
20	0.09	6.754e4	0.2183	4.7082	4.864e4	0.6612	5.0240	7.8	4.386e4	0.7879	5.0975	8.4	0.6
30	0.05	7.737e4	0.3270	5.1619	5.180e4	0.8120	5.4347	5.6	4.006e4	1.0688	5.5016	6.0	0.5
50	0.03	8.713e4	0.4570	5.6283	5.490e4	0.9722	5.8562	3.7	3.536e4	1.3862	5.9200	4.3	0.5
100	0.02	9.796e4	0.6147	6.1470	5.173e4	1.2610	6.3303	2.8	3.392e4	1.6437	6.3627	3.1	0.3
300	0.02	1.074e5	0.8697	6.8172	4.882e4	1.6111	6.9301	2.1	3.165e4	2.0041	6.9631	2.4	0.3
1000	0.02	1.080e5	1.1090	7.3047	4.807e4	1.8740	7.4288	2.1	3.122e4	2.2119	7.3549	2.4	0.3

Windhorst, Timmes, Wyithe et al. (2018, ApJS, 234, 41):

- 30–1000 M_{\odot} Pop III stars ($Z=0.00 Z_{\odot}$) live $\sim 10\times$ shorter than 2–5 M_{\odot} Pop III stars in their AGB stage.
- Hence, 2–5 M_{\odot} AGB companion stars can feed the LIGO-mass BHs left over from $M \gtrsim 30 M_{\odot}$ Pop III stars (assuming binaries in 2nd generation).

Table 3. Implied Red Giant Branch Pop III Star Observational Parameters Relevant to Caustic Transit Calculations

Mass ^a GB (M_{\odot})	T_{eff}^b (K)	Radius ^c (R_{\odot})	L_{bol}^d (L_{\odot})	M_{bol}^e (AB)	Bolo+IGM+K-corr ^f (AB-mag)			Giant Branch m_{UV}^g (AB-mag)			t_{rise}^h (hr)	transit ⁱ rate (/cl/yr)
					z=7	z=12	z=17	z=7	z=12	z=17		
1.0	6.999e3	3.25	22.8	+1.35	+4.83	+3.48	+2.96	55.42	55.41	55.73	0.63	9×10^4
1.5	1.181e4	2.13	79.7	-0.01	+0.91	-0.06	-0.53	50.13	50.51	50.88	0.41	1.0×10^3
2.0	1.611e4	1.78	191.	-0.96	-0.19	-1.01	-1.47	48.08	48.60	48.99	0.34	175.
3.0	2.311e4	1.53	598.	-2.20	-0.69	-1.39	-1.84	46.35	46.99	47.38	0.30	39.8
5.0	3.206e4	1.55	2.28e3	-3.66	-0.63	-1.25	-1.70	44.95	45.67	46.07	0.30	11.8
10	4.174e4	2.40	1.57e4	-5.75	-0.34	-0.92	-1.36	43.15	43.91	44.31	0.46	2.33
15	4.624e4	3.47	4.94e4	-6.99	-0.18	-0.74	-1.19	42.06	42.84	43.24	0.67?	0.87?
20	4.864e4	4.58	1.06e5	-7.82	-0.10	-0.65	-1.09	41.32	42.11	42.51	0.88*	0.44*
30	5.180e4	6.49	2.72e5	-8.85	+0.02	-0.53	-0.97	40.41	41.20	41.60	1.25*	0.19*
50	5.490e4	9.38	7.18e5	-9.90	+0.13	-0.42	-0.86	39.47	40.26	40.66	1.81*	0.081*
100	5.173e4	18.2	2.14e6	-11.09	+0.02	-0.53	-0.98	38.17	38.96	39.36	3.52*	0.024*
300	4.882e4	40.8	8.51e6	-12.59	-0.09	-0.65	-1.09	36.57	37.35	37.75	7.88*	0.006*
1000	4.807e4	74.8	2.68e7	-13.83	-0.12	-0.67	-1.12	35.29	36.07	36.47	14.44*	0.002*

- If $M \gtrsim 20 M_{\odot}$ Pop III RGB stars have $\mu \gtrsim 10^4 - 10^5$ during caustic transits, they could be detectable for a few months to $AB \lesssim 29$ mag with JWST.
- Note the combined Bolometric+IGM+K-corrections are more advantageous for Pop III RGB stars.

Table 4. Implied AGB Pop III Star Observational Parameters Relevant to Caustic Transit Calculations

Mass ^a AGB (M_{\odot})	T_{eff}^b (K)	Radius ^c (R_{\odot})	L_{bol}^d (L_{\odot})	M_{bol}^e (AB)	Bolo+IGM+K-corr ^f (AB-mag)			AGB m_{UV}^g (AB-mag)			t_{rise}^h (hr)	transit ⁱ rate (/cl/yr)
	— at Helium-depletion —				z=7	z=12	z=17	z=7	z=12	z=17	caust	rate
1.0	6.312e3 ^j	5.23 ^j	39.8 ^j	+0.74	+6.01	+4.57	+4.03	55.99	55.89	56.19	1.01	1.4×10^5
1.5	8.149e3	6.18	151.	-0.71	+3.36	+2.14	+1.64	51.89	52.01	52.35	1.19	4.0×10^3
2.0	1.145e4	4.66	335.	-1.57	+1.06	+0.07	-0.40	48.73	49.08	49.45	0.90	273.
3.0	1.736e4	3.56	1.03e3	-2.79	-0.36	-1.15	-1.60	46.09	46.64	47.03	0.69	28.9
5.0	2.658e4	2.89	3.74e3	-4.19	-0.72	-1.38	-1.82	44.33	45.01	45.41	0.56	6.43
10	3.938e4	3.03	1.98e4	-6.00	-0.42	-1.00	-1.45	42.82	43.57	43.97	0.58	1.71
15	4.215e4	4.55	5.88e4	-7.18	-0.33	-0.90	-1.34	41.73	42.50	42.89	0.88?	0.64?
20	4.386e4	6.14	1.25e5	-8.00	-0.27	-0.84	-1.28	40.97	41.74	42.14	1.19*	0.32*
30	4.006e4	11.7	3.17e5	-9.01	-0.40	-0.98	-1.42	39.83	40.59	40.98	2.26*	0.11*
50	3.536e4	24.3	8.32e5	-10.06	-0.55	-1.15	-1.59	38.63	39.37	39.77	4.70*	0.036*
100	3.392e4	44.0	2.31e6	-11.17	-0.59	-1.19	-1.64	37.49	38.22	38.61	8.50*	0.012*
300	3.165e4	101.	9.19e6	-12.67	-0.64	-1.26	-1.71	35.93	36.65	37.04	19.49*	0.003*
1000	3.122e4	163.	2.26e7	-13.65	-0.65	-1.28	-1.72	34.94	35.66	36.05	31.45*	0.001*

- If $M \gtrsim 20 M_{\odot}$ Pop III AGB stars have $\mu \gtrsim 10^4 - 10^5$ during caustic transits, they could be detectable for a few months to $AB \lesssim 29$ mag with JWST.
- Note the combined Bolometric+IGM+K-corrections are far more advantageous for Pop III AGB stars (especially at $z \gtrsim 12$)!

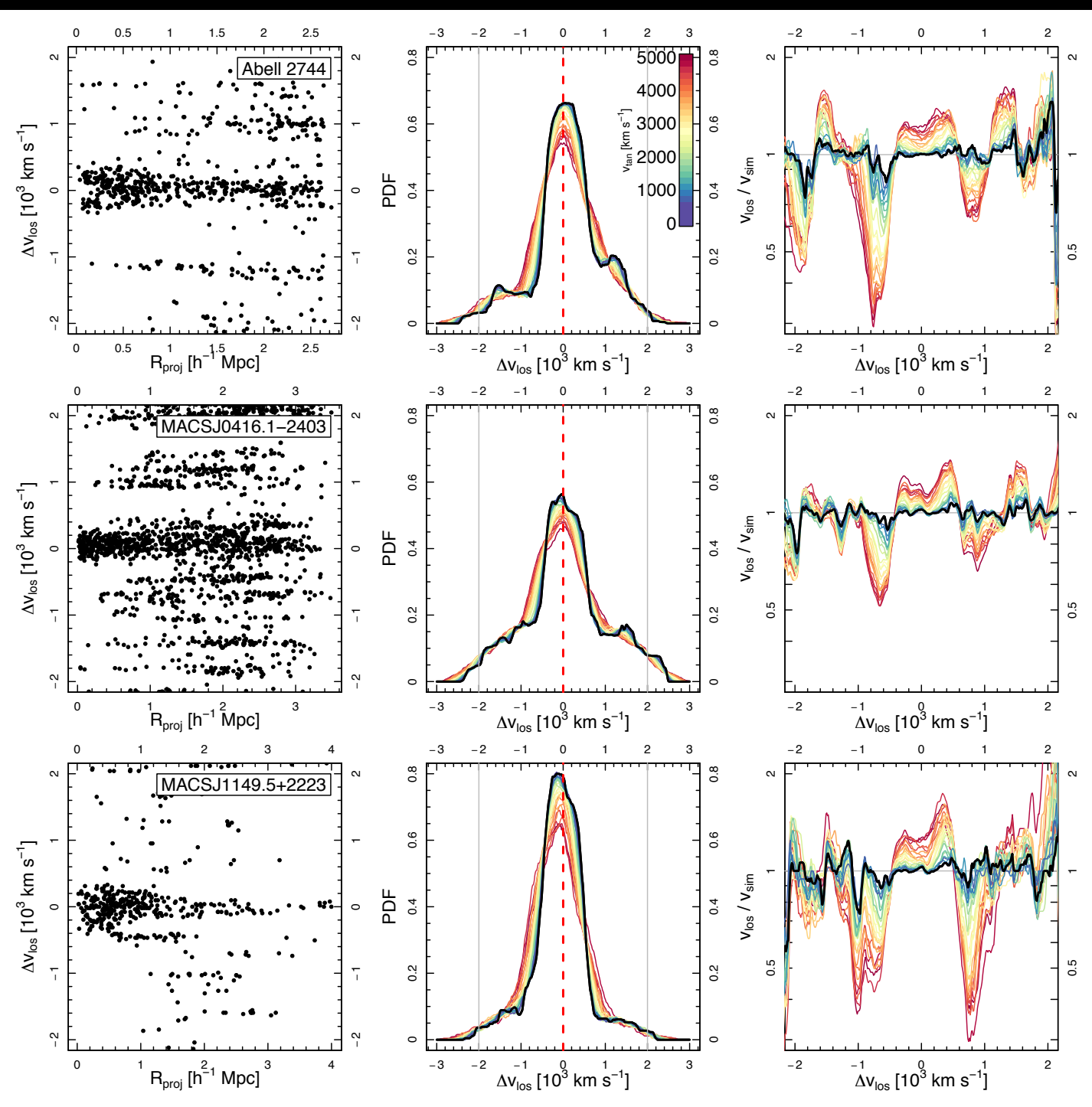
Table 5. Pop III Stellar Mass Black Hole Accretion Disk Parameters Adopted for Caustic Transit Calculations

Mass ^a	$M_{compact}$ ^b	R_s ^c	Radius ^d	L_{bol} ^e	M_{bol} ^f	bolo+IGM+K-corr ^g			m_{AB} -limits at ^h			t_{rise} ⁱ	Transit ^j	
ZAMS		BH	— of the UV accretion disk —			z=7	z=12	z=17	z=7	z=12	z=17	(z=12)	rate	
(M_\odot)	(M_\odot)	(km)	(R_\odot)	(L_\odot)	AB-mag	(AB-mag)			(AB-mag)			(hr)	(/cl/yr)	
BH accretion-disk bolometric luminosities and UV half-light radii scaling from microlensed quasars (Blackburne et al. 2011)														
30	~5.0 BH	15	1.4	$\lesssim 4.2 \times 10^4$	$\gtrsim -6.8$	-0.6	-1.4	-1.7	$\gtrsim 41.8$	$\gtrsim 42.4$	$\gtrsim 42.9$	0.27?	$\gtrsim 0.58?$	
50	~24 BH	72	3.0	$\lesssim 2.0 \times 10^5$	$\gtrsim -8.5$	-0.4	-1.2	-1.5	$\gtrsim 40.3$	$\gtrsim 40.9$	$\gtrsim 41.4$	0.58*	$\gtrsim 0.15^*$	
100	~65 BH	195	4.9	$\lesssim 5.4 \times 10^5$	$\gtrsim -9.6$	-0.2	-0.9	-1.3	$\gtrsim 39.4$	$\gtrsim 40.0$	$\gtrsim 40.5$	0.95*	$\gtrsim 0.06^*$	
300	~230 BH	690	9.2	$\lesssim 1.9 \times 10^6$	$\gtrsim -11.0$	-0.2	-1.0	-1.3	$\gtrsim 38.1$	$\gtrsim 38.6$	$\gtrsim 39.2$	1.8*	$\gtrsim 0.02^*$	
1000	~720 BH	2160	16.3	$\lesssim 6.0 \times 10^6$	$\gtrsim -12.2$	-0.2	-0.9	-1.3	$\gtrsim 36.8$	$\gtrsim 37.5$	$\gtrsim 37.9$	3.2*	$\gtrsim 0.01^*$	
BH accretion-disk bolometric luminosities and UV half-light radii estimated from multi-color thin-disk model														
30	~5.0 BH	15	1.9	$\lesssim 3.1 \times 10^4$	$\gtrsim -6.5$	-0.6	-1.4	-1.7	$\gtrsim 42.1$	$\gtrsim 42.8$	$\gtrsim 43.2$	0.37?	$\gtrsim 0.84?$	
50	~24 BH	72	4.5	$\lesssim 1.8 \times 10^5$	$\gtrsim -8.4$	-0.4	-1.2	-1.5	$\gtrsim 40.4$	$\gtrsim 41.1$	$\gtrsim 41.5$	0.87*	$\gtrsim 0.18^*$	
100	~65 BH	195	7.8	$\lesssim 5.9 \times 10^5$	$\gtrsim -9.7$	-0.2	-0.9	-1.3	$\gtrsim 39.3$	$\gtrsim 40.0$	$\gtrsim 40.4$	1.51*	$\gtrsim 0.06^*$	
300	~230 BH	690	15.8	$\lesssim 2.0 \times 10^6$	$\gtrsim -11.0$	-0.2	-1.0	-1.3	$\gtrsim 38.0$	$\gtrsim 38.6$	$\gtrsim 39.1$	3.1*	$\gtrsim 0.02^*$	
1000	~720 BH	2160	29.8	$\lesssim 6.6 \times 10^6$	$\gtrsim -12.3$	-0.2	-0.9	-1.3	$\gtrsim 36.7$	$\gtrsim 37.4$	$\gtrsim 37.8$	5.8*	$\gtrsim 0.01^*$	

● If $M \gtrsim 20 M_\odot$ Pop III stellar mass black hole accretion disks have $\mu \gtrsim 10^4 - 10^5$ during caustic transits, they could be detectable for a few months to $AB \lesssim 29$ mag with JWST. Rise times \sim hours–1 day; Decay times $\lesssim 0.4$ yr.

● Note the combined Bolometric+IGM+K-corrections are also more advantageous for Pop III stellar-mass black hole accretion disks.

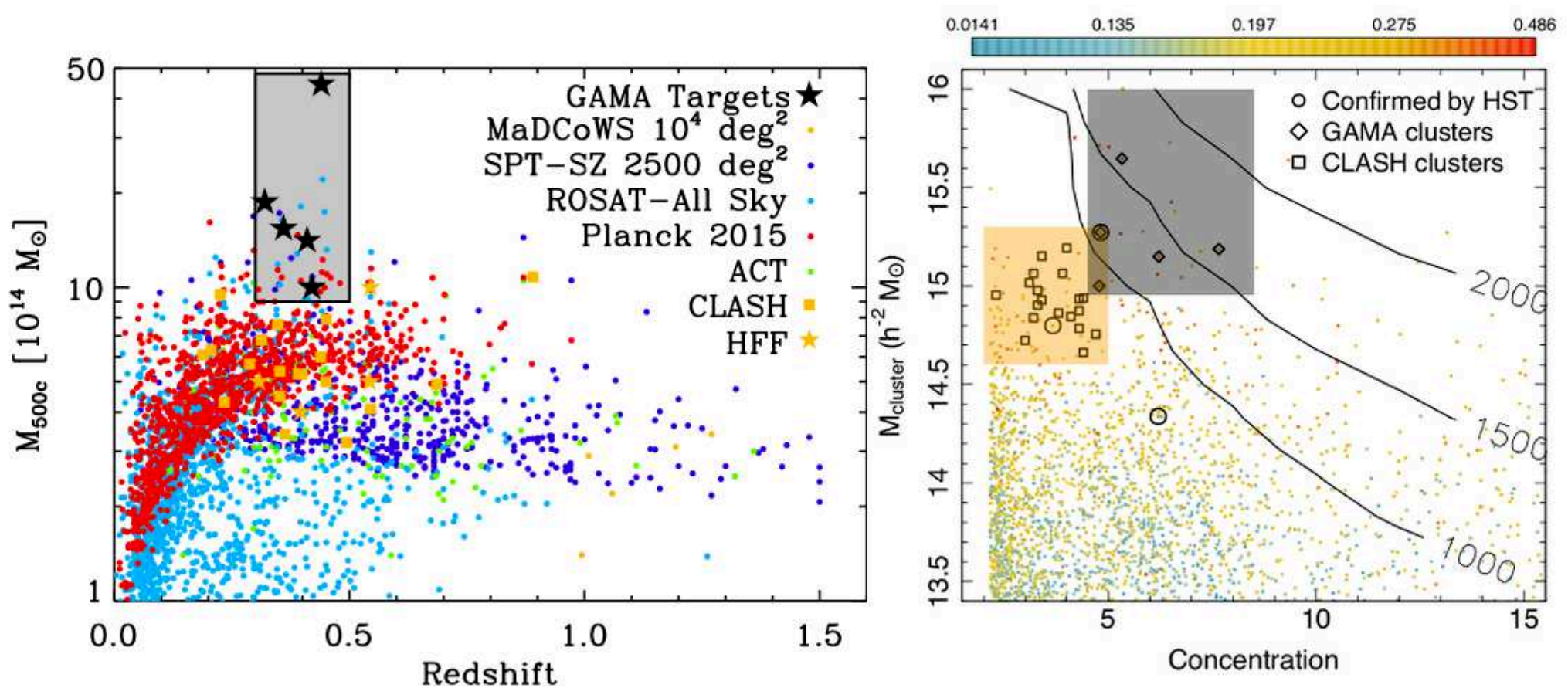
Multi- λ model: $T \propto r^{-3/4}$; $T_{max} \simeq 10 \left(\frac{M_{BH}}{100} \right)^{-3/8} \text{ keV}$; $r_{hl} \propto M_{BH}^{1/2}$.



Trumpet diagrams for JWST lensing clusters from ground-based spectroscopic $N(z)$ (Windhorst⁺ 2018):

- 1) Add random *space* velocity v_{sp} to clusters.
- 2) Projected v_T must be $\lesssim 1000 \text{ km/s}$ for v_{sp} not to unduly disturb radial $N(z)$.
- 3) Best clusters (Bullet) for caustic transits can have $v_T \lesssim 2700 \text{ km s}^{-1}$.

● JWST should monitor such clusters during its lifetime for caustic transits.



What are the best lensing clusters for JWST to see First Light objects?:

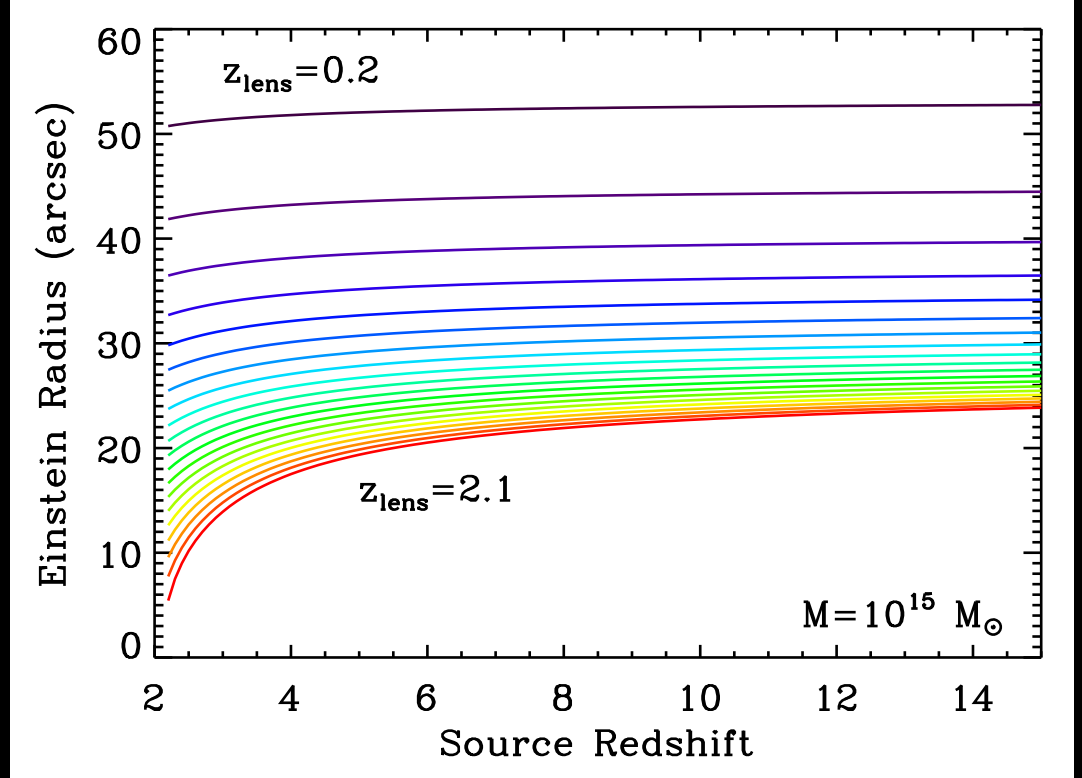
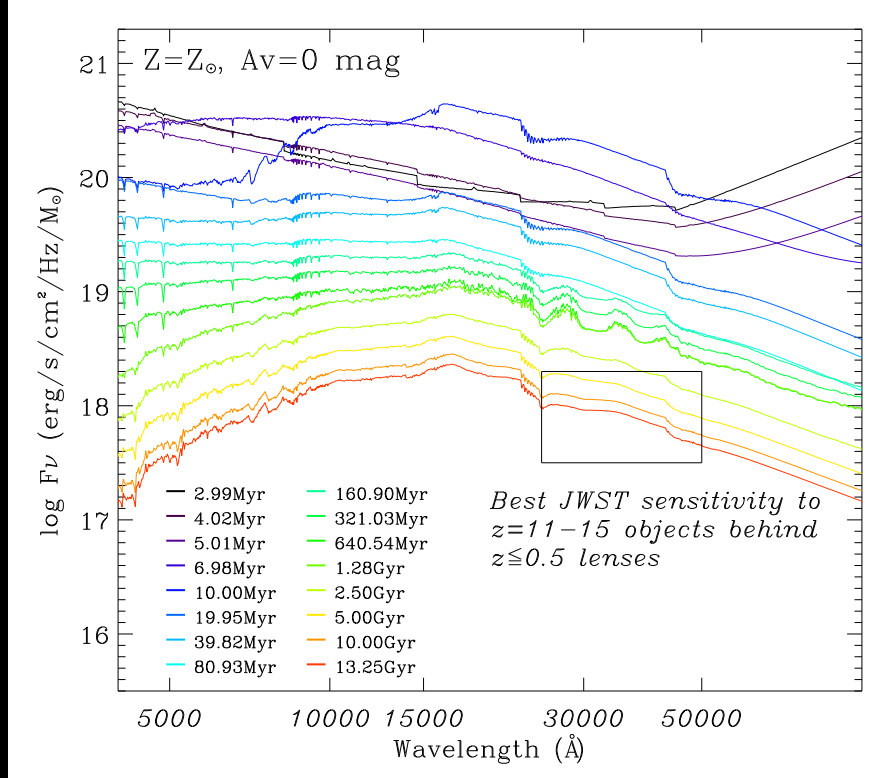
[LEFT] Best lensing clusters vs. ROSAT, Planck, SPT, MaDCoWS.

[RIGHT] Best lensing clusters compared to CLASH clusters.

(Contours: Number of lensed JWST sources at $z \simeq 1-15$ to $AB \lesssim 31$ mag).

● Resulting sweet spot for JWST lensing of First Light Objects ($z \gtrsim 10$):

Redshift: $0.3 \lesssim z \lesssim 0.5$; Mass: $10^{15} - 15.6 M_{\odot}$; Concentration: $4.5 \lesssim C \lesssim 8.5$



Galaxy SEDs for different ages: peak at $\lambda_{rest} \simeq 1.6 \mu\text{m}$ (Kim et al. 2017).

JWST-NIRCam peaks in sensitivity for $\lambda=3-5 \mu\text{m}$, where Zodi is lowest.

Sweet spot for lensing cluster $z \lesssim 0.5$: Zodi-gain mitigates $(1+z)^4$ -dimming.

- Minimizes effects from near-IR K-correction and ambient ICL.
- Lower redshift clusters also have higher (virialized) masses and much larger Einstein radii.
- This is critical for optimizing caustic transit detections away from ICL.

(3) What are the best lensing clusters to monitor caustic transits?

Unique compact lensing cluster CLIO 2863

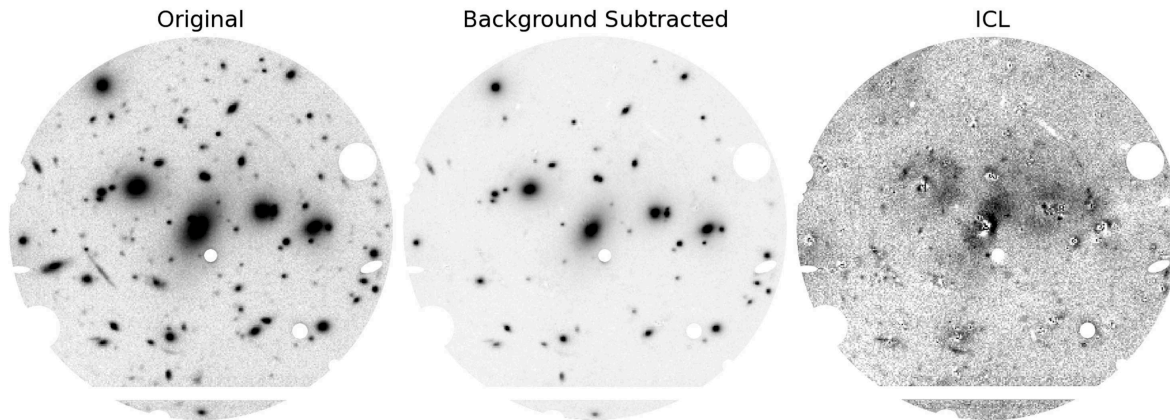
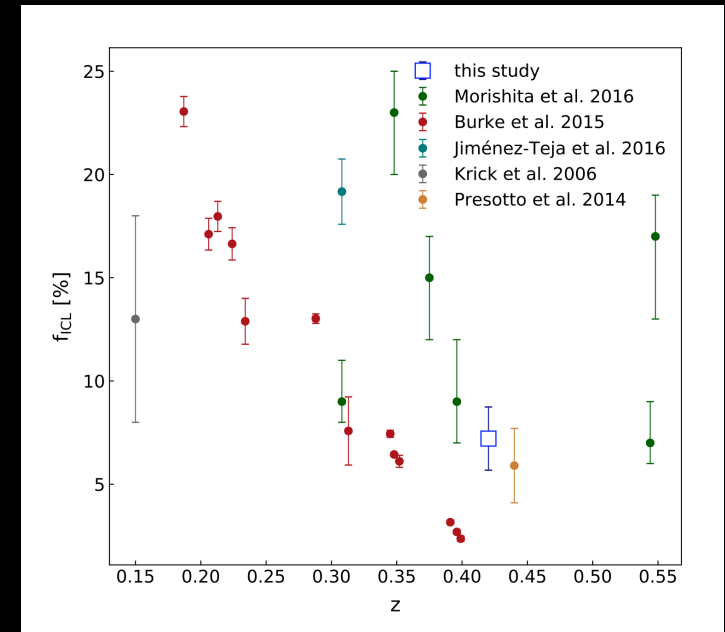
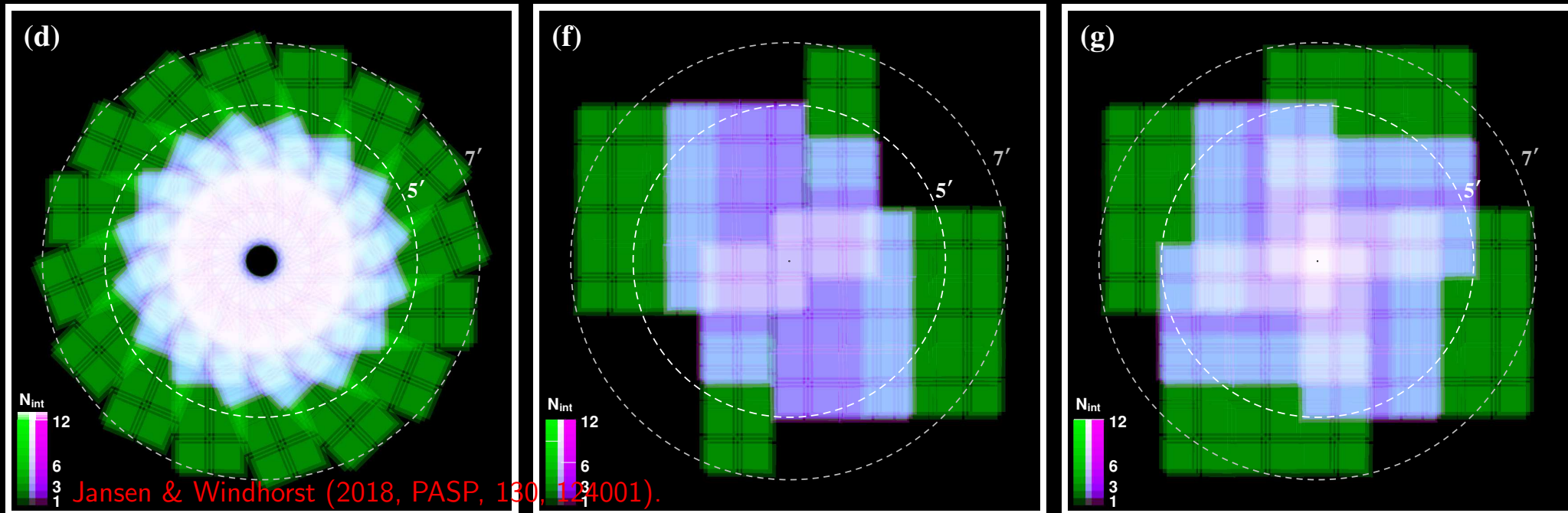


Figure 9. Visual representation of the full GALFIT modelling procedure. Left: Shows the original FORS2 r -band image with initial masking applied. Centre: Shows a cluster only residual after subtraction of the composite foreground and background galaxy GALFIT model. Right: Shows the residual ICL model after subtraction of the composite cluster model but before masking of the cluster member galaxy central regions.



Griffiths et al. (2018 MNRAS, 475, 2853): GAMA cluster at $z \simeq 0.42$ found through mass-concentration selection. Has 89 VLT MUSE members:

- Cluster has minimal ICL near the critical curves, optimal for caustic transit studies. Can see several arcs clearly in ground-based images.
- JWST should monitor clusters with minimal ICL near the critical curves to minimize microlensing and maximize caustic transit magnifications.



[LEFT]: Example of 16-epoch extension. Alternatively:

[MIDDLE]: 4-epoch filled NIRCcam + NIRISS Windmill mosaic.

[RIGHT]: 4-epoch extended NIRCcam + NIRISS Windmill mosaic.

- GO's can repeat NIRCcam primaries + NIRISS parallels as often as needed during JWST's 5–14 year lifetime at *any* PA — no ORIENT restrictions!
- NEP yields time-domain imaging to $AB \lesssim 29$ mag.
- NEP provides robust multi-ORIENT grism spectra to $AB \lesssim 28$ mag.